



# A critical review in the features and application of photocatalysts in wastewater treatment

Aref Shokri<sup>1</sup> · Mahdi Sanavi Fard<sup>2</sup>

Received: 29 January 2022 / Accepted: 26 April 2022 / Published online: 28 May 2022  
© Institute of Chemistry, Slovak Academy of Sciences 2022

## Abstract

Rapidly escalating environmental contamination is considered as the most urgent challenge over the world which between them, water contamination is the top priority. As a result, the return of investment on developing novel methods for the effective removal of various kinds of unfavorable contaminants from wastewater would be enormous. In view of the current scenario, among different branches of AOPs for wastewater treatment, the photocatalytic process has emerged as an effective and highly promising technology. The ability to remove pollutants from various environments, the formation of nontoxic products, demand minimum chemicals at a reasonable time, effective degradation, generation of the minimum by-products as pollutants, and energy-efficient operation are some of the major advantages of the photocatalytic process. However, because of several serious challenges concerned with the semiconductor metal oxides, the performance of the solar photocatalyst is still inadequate. As a result, the photocatalyst method is facing some serious challenges, including material instability, ineffective charge transformation and separation, and a discrepancy between solar spectrum and semiconductors' bandgap, which needs to be further explored. In this review paper, photocatalyst doping, coupling, doping with nonmetal, transition metals, noble metals, and co-doped are investigated as methods for enhancing process efficiency. Moreover, developing some immobilized nanocatalyst systems for fixing semiconductors are briefly discussed. Integrated photocatalyst absorbents as an effective method for overcoming some significant shortcomings of individual photocatalyst besides standards for selection of major adsorbents like graphene, clays, zeolite, and activated carbon are investigated. In addition, several crucial parameters that have demonstrated substantial influence on governing the photocatalytic mechanism are discussed. The main parameters for evaluating process effectiveness are summarized. Finally, different serious challenges associated with the photocatalyst method, some strategies for improving photocatalytic activity besides proposing future research direction, and critical recommendations for addressing those challenges are discussed to further broaden the horizon of such a promising method.

**Keywords** Bandgap · Electron–hole pairs · Hydroxyl radical · Photocatalytic method · Wastewater treatment

## Introduction

Recently, because of growing stringent standards over the world for the remediation of wastewater and also the severe restrictions on water resources, the researcher's attempt is highly concentrated on different water treatment methods, practical water reuse approaches and elimination of perilous organic components. Different types of materials have been

utilized to eliminate the pollutants from wastewater, such as ozone, various kinds of adsorbents, a membrane made from organic and inorganic materials, and homogenous and heterogeneous catalyst (Saleh 2016; Schollée et al. 2021). Moreover, to remediate different types of wastewaters, previous researchers have made considerable attempts by utilizing traditional approaches like biological, chemical, and physical methods. Biological remediation is defined as eliminating a pollutant by the metabolic interactions of living organisms, including different kinds of fungi and bacteria which present in water and soil. In this process, the chemicals are decomposed by microorganisms to smaller species. Currently, the demand for traditional pollutants elimination methods is drastically decreasing, although they have demonstrated good efficiency. Nevertheless, the conventional methods

✉ Aref Shokri  
aref.shokri3@gmail.com

<sup>1</sup> Jundi-Shapur Research Institute, Dezful, Iran

<sup>2</sup> Department of Chemical Engineering, Tafresh University, Tafresh, Iran

have their own limitations like slow and complicated operations, high operational costs, and low removal effectiveness. During some conditions, they show less flexibility toward a broad range of different types of organic components (Tekin et al. 2018; Shokri 2020). Some of the typical drawbacks of the traditional methods are the following (a) conversion from one organic removal compartment to another one can highly decrease the process efficiency (Klauck et al. 2017), (b) due to slow removal rates, the removal process requires huge volumes of storage tank (Srinivasan and Viraraghavan 2010), and (c) non-devastating feature, usually generate a massive quantity of slug which require to the additional treatment process. Also, the traditional water treatment approaches that are available today do not completely remove or degrade the contaminants. Therefore, the advent of a proper alternative water treatment approaches that can absolutely remove or degrade such pollutants is significantly at a premium.

Nowadays, different investigations have been conducted to explore novel methods and reduce the downsides of previous ones. In order to eliminate ions and organics, several sophisticated techniques that depend on the utilization of heterogeneous compounds have been employed in the last decades (Huang et al. 2017, 2018b). For instance, nanomaterial modification has to turn into an effective method in the adsorption process, which is developing from the integration of usual nanoparticles and various modifiers (Huang et al. 2018c; Liu et al. 2018; Zeng et al. 2018). Mussel-inspired chemistry is regarded as one of the new and simple approaches for functionalizing different materials like nanoparticles and surface modification in order to generate multifunctional compounds. The significant focus is due to long-term stability, adaptability, smooth and easy operation, and efficacious modification (Liu et al. 2015). Polydopamine or dopamine cohesion to solid substrate surface primarily is related to the coating or modification process (Huang et al. 2018a). Recently in the biological remediation, a nitrifying-enhanced activated sludge was utilized by the addition of ammonium into the traditional activated sludge in order to decrease sludges in the membrane bioreactor and membrane bio-fouling phenomenon. The outcomes showed that the filterability rate increased 2.5 times more than the traditional activated sludge by using nitrifying-enhanced activated sludge. Also, membrane fouling was decreased because of extracellular polymeric materials and the low formation of soluble microbial products (Sepahri and Sarrafzadeh 2018).

For the contaminants treatment in wastewaters and facilitate the pollutants degradation or elimination by redox processes, advanced oxidation processes (AOPs) were emerged. They utilize hydroxyl radicals ( $\text{OH}^\bullet$ ) and other powerful oxidants by indirect and direct operations to effectively remove the refractory organic contaminants. Hydroxyl radicals due to having a huge standard potential ( $E^\circ(\text{OH}^\bullet/\text{H}_2\text{O}) = 2.80 \text{ V/SHE}$ ) are considered one of the most strong

oxidizing factors, which makes them interact non-selectively with a broad range of contaminants to produce dehydrogenated and hydroxylated products until their mineralization process (changing to inorganic ions, water, and carbon dioxide) (Shokri and Fard 2022). In other words, because of the powerful non-selective oxidative feature of  $\text{OH}^\bullet$ , it is approximately mineralized and oxidized any organic molecule, which finally leaving carbon dioxide and inorganic ions (Shokri and Mahanpoor 2016). Catalysts like Fenton reagent, zinc oxide, and titania, energy sources like heat, ultrasonic, and ultraviolet light, or oxidants such as  $\text{O}_3$  and  $\text{H}_2\text{O}_2$  are used for the generation of  $\text{OH}^\bullet$  (Shokri 2019). Between different AOPs like ultrasound, electrochemistry, ozonation, Fenton, etc., the photocatalytic method is highly promising to the researchers due to various properties which demonstrate its enormous potential for effective contaminant degradation. Following are some of the major advantages: (a) formation of nontoxic products, (b) broad range of organics degradation, (c) ability to eliminate pollutants from various environments, (d) generation of lowest by-products as pollutants, (e) energy-efficient operation and (f) requiring lowest amount of chemicals with the moderate state at an appropriate time (Pang et al. 2021).

The photocatalyst method had emerged when Fujishima and Honda, during their works in 1972, had found a valuable inorganic compound, namely, titanium dioxide ( $\text{TiO}_2$ ). Primarily, in order to water splitting into  $\text{O}_2$  and  $\text{H}_2$  in a photo-5 electrochemical cell, titanium dioxide was utilized. The discovery of titanium dioxide has driven many researchers to investigate the utilization of titanium dioxide in different fields, specifically in photocatalyst. In 1991 Bahnemann and his colleagues were utilized  $\text{TiO}_2$  suspensions for the purpose of wastewater treatment, which is considered the primary research on the photocatalysis method (Bahnemann et al. 1991). They reported the effect of pH, temperature, and light intensity alongside utilizing titanium dioxide photocatalyst suspensions on the degradation rates of halogenated hydrocarbons. As a result, they realize that photocatalyst could be a highly promising approach for the wastewater treatment and still required to be precisely investigated in order to further enhance it. Hence, following that many research efforts has been performed by utilizing titanium dioxide as a photocatalyst.

Various types of semiconductors have been utilized as photocatalysts for the photocatalytic degradation of organic and inorganic pollutants (Chen et al. 2016). Because titanium dioxide possesses attractive advantages like cost-effectiveness, availability, stable chemical structure, and harmless nature, it is extensively investigated for photocatalytic purposes (Rostami et al. 2019). Despite the aforesaid benefits, because of its inherent properties like broad bandgap around 3.2 eV and low quantum effectiveness, which restricts the application of titanium dioxide

in visible light, the viable utilization of photocatalytic  $\text{TiO}_2$  has been limited (Rostami et al. 2019). One crucial method is to change the nanomaterial to improve visible light absorption in order to improve the solar photocatalyst performance during solar radiation. In order to decrease the titanium dioxide bandgap and stimulate it by direct sunlight radiation or visible light, different types of doping are presented. Moreover, various investigations have been concentrated on designing and enhancing the single-phase oxide photocatalyst like perovskite-kind oxide, which is efficiently performed during the irradiation of visible light (Saleh 2018).

Some photocatalysts can adsorb pollutants other than their degradation mechanisms. The adsorption method, because of its effectiveness, economic features, simplicity, and uninfluenced by toxicity, is one of the effective treatment options for contaminants removal (Saleh 2018). Although this approach to some extent concentrates the contaminants by absorption and then separation from the process, however, it is incapable of totally removing or degrading the contaminants when individually employed. Different adsorbents have been reported in the literature for the removal of contaminants like polymeric adsorbents, zeolite, clays, and activated carbon (Zhu et al. 2016). During the adsorption-dependent removal method, activated carbon has been a perfect option for some contaminants. Many adsorbents were used as a base for photocatalysts to enhance their efficiency. In this way, graphene oxide (GO) can be used as good support for  $\text{TiO}_2$  photocatalyst for degradation of persistent pollutants (Shokri et al. 2016).

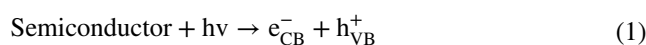
The major disadvantage of photocatalyst nanoparticles is that with application in a slurry condition, the accumulation of them will cause a drastic reduction in photocatalytic efficiency (Saleh et al. 2017; Alansi et al. 2018). Moreover, the polar and non-permeable surface of the photocatalyst will lead reduction in the adsorption of the contaminants on its surface; as a result, decreasing the photodegradation efficiency. In order to overcome this challenge, new investigations for immobilizing the photocatalyst on adsorbents like zeolite, clays, carbon are the focus of attention. By integrating photocatalyst and adsorbents, an adsorbent that decomposes toxic organic materials could be generated in the presence of ultraviolet or visible light irradiation (Peng et al. 2016). This synergistic integration does not only overcome major disadvantages, like rapid photogenerated electrons recombination and low absorptivity but also, maintains all of the attractive attributions of both individual compounds (Tian et al. 2022). In comparison with the slurry condition, immobilizing photocatalyst on adsorbents is desirable since it will facilitate the integrated photocatalyst adsorbent separation from bulk solution in order to reusing photocatalyst (Yahya et al. 2018b).

The investigation on combining the photocatalyst alongside adsorbents was initiated in 1999 when Burns and his colleagues suggested fouling avoidance methods for  $\text{TiO}_2$  catalyst (Burns et al. 1999). Inspired by their accomplishments, many investigations in integrated photocatalyst adsorbents have been implemented, and under visible light irradiation, degradation efficiency higher than 98% for 18 min has been detected (Fan et al. 2016). However, a few investigations have been done in this region. As a result, it still needs further exploration to harness its real potential.

In this review paper, the authors study the overview of the photocatalyst method for wastewater remediation concerning semiconductors and different doping types like metal doping, nonmetal doping, transition and noble metal doping, co-doped, and coupling. Moreover, catalyst fixation, integrated photocatalyst adsorbents, and criteria for selection of proper adsorbents are investigated. Following that, significant parameters that govern the photocatalyst process, challenges, and methods for overcoming them are comprehensively studied. Finally, the authors critically present their suggestions to clearly delineate future research direction to considerably widen the application of this green technology and bridge the knowledge gaps.

## Semiconductor

Semiconductors are considered as the integral parts of photocatalyst process, which have a conduction band (CB, with higher energy and without an electron) and a valence band (VB, with full electrons) with a certain bandgap. The absorption of the light photons by semiconductors and following that the generation of electron ( $e^-$ ) holes ( $h^+$ ) in the VB is the fundamental mechanism of the photocatalytic method. According to Eq. (1), ( $e^-$ ) is excited from the VB to the CB, as a result generating an electron–hole pair. According to Eq. (2), the excited electrons can interact with electron acceptors like oxygen which is dissolved in water or presented on the catalyst surface and reduce it to  $\text{O}_2^-$  (Karimi and Shokri 2021). According to Eqs. (3) and (4), the holes can scavenge OH and  $\text{H}_2\text{O}$  molecules on the surface of the nanoparticle to produce  $\text{OH}^\bullet$ . According to the Eq. (5),  $\text{OH}^\bullet$  possessed significant oxidizing ability (Rahmani et al. 2019), which is excited and has great potential to efficiently mineralize any organic compounds which are adsorbed onto the particle surface to produce  $\text{CO}_2$  and  $\text{H}_2\text{O}$ . Figure 1 simply demonstrates the photo-induced operation.



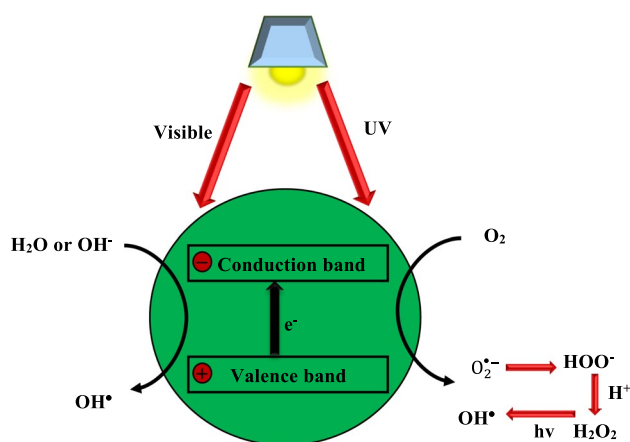
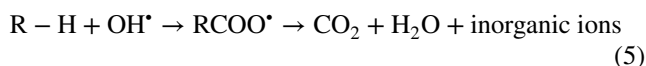


**Fig. 1** Schematic illustration of the photochemical semiconductor activation and the hydroxyl radical generation. (Akerdi and Bahrami 2019)



Previously, nano-semiconductors like ZnS, ZnO, Fe<sub>2</sub>O<sub>3</sub>, SiO<sub>2</sub>, CdS, TiO<sub>2</sub>, etc., have been utilized extensively to overcome several environmental challenges by several processes like sensors, water splitting, solar cell, etc. (Qin et al. 2017). Some critical semiconductor features are: (a) photo-reacting, (b) stability concerning light corrosion, biological and chemical processes, (c) significant sensitivity toward visible light and ultraviolet, (d) cost-effectiveness, and (e) non-toxicity (Bonigari et al. 2018). In comparison with the other approaches, semiconductors in the photocatalytic process can be more economic due to their low preparation cost, hard-wearing feature, being cheap and unsophisticated and easy operational process, no sludge formation (by-product contaminant) at the end of the treatment process, without requiring for addition of secondary chemical, utilizing clean energy resources such as low energy consuming light bulbs and sunlight, and reaching higher performance by employing a low quantity of semiconductors. Total contaminant mineralization and elimination can be occurred by application of a semiconductor in photocatalytic operation. Nevertheless, in some approaches, pollutants are only changed from one type to another one, hence adding an extra treatment process which is not economically practical.

The size of the particle can be regarded as a significant element to improve the photocatalytic efficiency of

semiconductors since it can enhance the energy gap of VB-CB and the recombination of electron-hole. The growing application of nanomaterials in wastewater treatment is because of their better physical and chemical properties like dimensions of less than 100 nm and huge surface area (Shokri et al. 2017; Radhika et al. 2019). Some chemical and morphological modifications like the addition of appropriate material to semiconductor design, increasing porosity, and surface area have been utilized in order to enhance the photocatalyst efficiency of semiconductors (Akerdi and Bahrami 2019).

Nevertheless, engineering and nanoscience enhancements open up an opportunity to offer more economic and eco-friendly methods for nanoparticles generation with certain properties. A significant increase in photocatalytic performance, especially in UV, is due to remarkable morphological and physical modification. As a result, although chemical modification causes activation of semiconductors in the visible area, the modified nanoparticle demonstrated the considerable potential to decrease recombination, one-dimension electrical charges transformation, and controllable porosity (Saghi et al. 2018). Table 1 summarizes the generation of various semiconductor morphologies such as nanotubes, nanoporous/mesoporous, nanorod, nanowire, nanofilm, nanoneedle, and nano-disk.

Lower recombination and considerable electron mobility will be obtained due to decreasing intercrystalline tangency in one-dimensional nanomaterials and the availability of one channel for electron movement. The semiconductor's physical form will modify by alternating specific experimental factors, like the properties of supplementary material, precursor rate, time, and temperature of the reaction. Van et al., reported that because of significant surface area and tiny particle size, mesoporous CdS nanoparticles had demonstrated a higher ratio in photocatalytic hydrogen formation compared with cubic CdS and bulk CdS (Van et al., 2022). As an effective and rapid approach for methyl orange removal utilizing spherical cobalt and nickel nanoparticles as the catalyst, hollow nickel nanoparticles and hollow cobalt nanoparticles were investigated (Sha et al. 2016). The outcomes showed that the hollow cobalt nanoparticles demonstrated the highest degradation rate.

## Photocatalyst doping

In terms of the energy and environmental challenges, efficiently harnessing sunlight as an unlimited energy resource is highly beneficial. Around 40% of sunlight includes visible photons, while only 4–5% of it is in the ultraviolet zone (Alamelu and Jaffar Ali 2018). Generally, semiconductors have a broad bandgap, with optical absorption in the ultraviolet zone, which is less than 400 nm. Many investigations

**Table 1** Nanostructure materials with various morphologies utilized as semiconductors

| Semiconductor   | Target wastewater                | Morphology    | References                  |
|-----------------|----------------------------------|---------------|-----------------------------|
| $Cd_xZn_{1-x}S$ | Methylene blue                   | Mesoporous    | Lee et al. (2017)           |
| $TiO_2$         | Methyl orange                    | Nanotube      | Smith et al. (2009)         |
| PANI/ $BiVO_4$  | Rhodamine (RhB), and phenol      | Spindle-like  | Shang et al. (2009)         |
| $TiO_2$         | Eosin B                          | Thin film     | Zhou and Ray (2003)         |
| N/F- $TiO_2$    | Methyl orange                    | Nanobelts     | He et al. (2012)            |
| $ZnIn_2S_4$     | Congo red, and rhodamine B       | Marigold-like | Chen et al. (2009)          |
| ZnO             | Multiple xenobiotics             | Nanowires     | Rogé et al. (2018)          |
| BiOI            | p-chloroaniline                  | Nanosheet     | Li et al. (2017b)           |
| Co/Ni           | Methyl orange                    | Hollow        | Sha et al. (2016)           |
| BiOI            | 2,2-bis(4-hydroxyphenyl) Propane | flower-like   | Lan et al. (2017)           |
| $Bi_2WO_6$      | Binary mixture                   | Thin film     | Zargazi and Entezari (2019) |
| ZnO/CuO         | Three different dyes             | Thin film     | Ghosh and Mondal (2015)     |
| ZnO             | Rhodamine B                      | Nano disks    | Seo and Shin (2015)         |
| ZnO             | Methyl orange                    | Needle-shaped | Khalid et al. (2015)        |
| $TiO_2$         | Reactive black dye               | Thin film     | Stambolova et al. (2012)    |

have been conducted to improve the photocatalyst performance of semiconductors within the range of visible light by utilizing different types of materials with a limited bandgap or integration of various compounds in the design of semiconductors to make the absorption process possible in the infrared or visible area, like coupling with crystal anisotropic growth, dyes, ions and other semiconductors (Nguyen et al. 2018). Moreover, activation using visible light prevents recombination of excited electron–hole pairs.

### TiO<sub>2</sub> and doped-TiO<sub>2</sub>

In order to select the proper photocatalyst, the value of the bandgap is of significant importance. Typically, due to the limited bandgap, especially between 1.4 and 3.8 eV, semiconductors are desired to perform as photocatalysts (Jing et al. 2022). Significant advantages like eco-friendliness, non-toxic nature, significant chemical stability, cost-effectiveness, and availability make titanium dioxide one of the highly appropriate photocatalysts (Zhang and Chu 2022). The broad bandgap is considered as the significant shortcoming of  $TiO_2$  as a photocatalyst. The absorption of a little part of the ultraviolet area is due to the aforesaid reason (Shokri 2020). Some researchers investigated the bacterial decomposition and observed that titanium dioxide is a proper photocatalyst however cannot be utilized in visible light, which results in low quantum performance (Qin et al. 2015). Because of the broad bandgap around 3.2 eV, absorption in natural sunlight is restricted (Alamelu and Jaffar Ali 2018). A higher bandgap would need higher energy to initiate the photocatalyst, whereas titanium dioxide only presents an absorption wavelength of less than 400 nm. As a result, because of these significant disadvantages, as shown

in Table 2, the researchers have observed various approaches to overcome the aforesaid downside by incorporating the transition metal and nonmetal doping.

Based on the different observations, the approach utilized for the preparation of doped titanium dioxide has considerable influence on the catalytic properties and efficiency. There are different available approaches to the preparation of doped titanium dioxide like co-precipitation, hydrothermal hydrolysis, and solgel (Malengreaux et al. 2017). The sol–gel process is considered a conventional approach to integrating doped titanium dioxide. In order to prepare nanomaterials, the sol–gel method utilized simple processes and devices. This method has been employed in different applications like chemical sensors, catalysis, membrane technology, etc. (Tong et al. 2014). In order to calculate the methyl orange degradation rate, Zhou et al. (2010) integrated vanadium doped titanium dioxide using the sol–gel approach and added  $Ti(OBu)_4$  as a precursor (Zhou et al. 2010). Then, Nguyen-Phan et al. integrated Lanthanum-doped titanium dioxide by utilizing the sol–gel approach integrated with the supercritical fluid drying approach. The integration of both approaches generates homogenous tiny size crystals (Nguyen-Phan et al. 2012).

Apart from the sol–gel approach, the hydrothermal approach is another solution for preparing doped titanium dioxide. Khan and Cao (2013) have been integrated a single doped of yttrium (Y) with titanium dioxide by hydrothermal approach. By decreasing the bandgap, a homogenous size of crystal was generated, which accordingly improved the photocatalytic activity during the visible light radiation. Khalid et al. (2015) prepared titanium dioxide with C-Y-co-doped by hydrothermal approach, and because of tiny



**Table 2** Titanium dioxide doping to limited bandgaps

| Transition metal or nonmetal doping        | Main results                                                                                                                                                                                                  | References                 |
|--------------------------------------------|---------------------------------------------------------------------------------------------------------------------------------------------------------------------------------------------------------------|----------------------------|
| Nitrogen-doped TiO <sub>2</sub>            | In comparison with pure TiO <sub>2</sub> , nitrogen-doped TiO <sub>2</sub> demonstrated higher photocatalytic activity in visible light illumination against azo dye Orange G                                 | Sun et al. (2008)          |
| Yttrium(Y)-doped TiO <sub>2</sub>          | In comparison with individual TiO <sub>2</sub> , Y-doped TiO <sub>2</sub> improved photocatalytic activity and increased separation of electron–hole pairs, besides reducing amounts of the bandgap           | Khan and Cao (2013)        |
| Cerium dioxide-doped TiO <sub>2</sub>      | Bandgap decreased from 3.29 to 3.15 eV                                                                                                                                                                        | Plodinec et al. (2014)     |
| Chromium (III) ions-doped TiO <sub>2</sub> | In comparison with pure TiO <sub>2</sub> , photocatalytic activity enhanced, and during ultraviolet and VB irradiation, optimal concentrations of dopants are 0.15% and 0.12% against degradation of XRG dyes | Yadav et al. (2016)        |
| Zinc-doped TiO <sub>2</sub>                | In comparison with individual TiO <sub>2</sub> , degradation of nitrobenzene by utilizing Zn doped TiO <sub>2</sub> was 99%                                                                                   | Reynoso-Soto et al. (2013) |
| Carbon-Yttrium-co-doped TiO <sub>2</sub>   | In comparison with single doped titanium dioxide, C-Y-co-doped titanium dioxide demonstrated the maximum absorbance rate, which was 405 nm                                                                    | Khalid et al. (2015)       |
| Lanthanum-doped TiO <sub>2</sub>           | In comparison with individual TiO <sub>2</sub> , the optimal concentration of dopant was 0.02 mol% La-TiO <sub>2</sub> and in photocatalytic activity enhanced by 30.7%                                       | Qing and Rui-Zhi (2012)    |
| Vanadium(V)-doped TiO <sub>2</sub>         | The absorption boundary is moved from 380 to 650 nm                                                                                                                                                           | Zhou et al. (2010)         |
| Sulphur-doped TiO <sub>2</sub>             | In comparison with individual TiO <sub>2</sub> , during radiation at a wavelength over 440 nm efficiency of methylene blue degradation for doped TiO <sub>2</sub> was significant                             | Ohno et al. (2004)         |
| Chromium (III) ions-doped TiO <sub>2</sub> | With the increasing quantity of doped content quantity of eV reducing                                                                                                                                         | Malengreaux et al. (2017)  |
| Forum (III) ions-doped TiO <sub>2</sub>    | With the increasing quantity of doped content quantity of eV reducing                                                                                                                                         | Malengreaux et al. (2017)  |

crystallite size and increased visible light absorption, doped photocatalyst activity and co-doped samples were increased.

Moreover, for preparing doped TiO<sub>2</sub>, the co-precipitation approach can be used. Zuas et al. (2014), by utilizing the co-precipitation approach, have combined cerium dioxide (CeO<sub>2</sub>) and detected that the catalyst has a lower bandgap ranging from 3.29 to 3.15 eV. Furthermore, for wide-ranging applications co-precipitation method shows much promise.

Recent investigations have integrated hydrothermal approaches along with other approaches. Zhu et al. (2006) integrated Cr<sup>3+</sup> doped titanium dioxide by integration of sol–gel and hydrothermal approaches. Both approaches are crucial as they provide specific advantages in the dopant solution. For the hydrothermal approach, it facilitates dopant transitional metal distribution in titanium dioxide and avoids the formation of heterogeneous metal oxides phases, while for the sol–gel approach, it promotes the charge carrier transmittance and the bulk trap (Zhu et al. 2006).

Few parameters have been demonstrated to have considerable impacts on improving photocatalytic activity. One parameter is the degree of dopant concentration. This parameter would result in increasing the photocatalytic activity and, as a result, increasing the contaminants degradation performance.

Moreover, Vanadium-doped titanium dioxide provided by Zhou et al. (2010) demonstrated that the dopant concentration affected the photocatalytic activity, in which a higher concentration of dopant ions will reduce the bandgap value

(Zhou et al. 2010). Malengreaux et al. (2017) adjusted single doped chromium and ferric and detected that increasing the number of dopants reduces the bandgap value. In contrast, rather than the increasing amount of dopants, the optimal quantity of dopant concentration is crucial to enhance the photocatalyst activity. According to the different investigations, lower amounts of concentration cannot improve, whereas additional concentration will finally decrease the photocatalytic activity. Increasing dopants over 5% will be decreased the photocatalytic activity (Malengreaux et al. 2017).

Apart from dopant concentration, by the presence of anatase, calcination temperature can affect photocatalytic activity. Ohno et al. (2004) investigated its influence on titanium dioxide with sulfur doping. According to the experimental results, a temperature of 500 °C for calcination temperature was detected to be the optimized temperature at which the most powerful photocatalytic absorption occurs in the visible region. At a temperature higher than 500 °C, the anatase formation was decreased and enhanced to the rutile phase. In contrast, extra investigation considering the influence of calcination temperature on carbon-doping with titanium dioxide showed that for photocatalytic activity, the optimized temperature is 400 °C (Lin et al. 2013).

For co-doped with titanium dioxide that includes Eu<sup>3+</sup>-Fe<sup>3+</sup> and La<sup>3+</sup>-Fe<sup>3+</sup>, amounts of the bandgap are heavily affected by the presence of ferric (Malengreaux et al. 2017). Zhu et al. (2006) utilized FeCl<sub>3</sub> and FeCl<sub>2</sub> as the

initial materials to integrate single doped titanium dioxide and detected the presence of ferum ion affected the photocatalytic activity rather than the presence of chloride ion, which does not show any significance.

The pH values have a considerable impact on the photocatalyst activity, apart from the dopant's concentration. Reynoso-Soto et al. (2013) integrated zinc-doped titanium dioxide and demonstrated 90, 99, and 10% degradation performance for nitrobenzene (NB), including pH values of 10, 7 and 4, respectively. The outcomes showed that although in the acidic environment, NB can efficiently degrade, in the alkaline environment, little conversions were detected, which is because of the zeta potential of Zn-doped titanium dioxide that performs as a powerful Lewis because of positive surface charges.

### Coupling

Using the band coupling between the limited-bandgap semiconductor such as CuO, Fe<sub>2</sub>O<sub>3</sub>, CdS, and In<sub>2</sub>O<sub>3</sub> and broad-bandgap semiconductors like titanium dioxide and zinc oxide, the effective separation and transformation of photogenerated electrons will occur (Ravichandran et al. 2016). The system for the charge transformation mechanism contributed to a coupled semiconductor process, and the mechanism of decreasing the CB and VB in a semiconductor is demonstrated in Fig. 2. Several investigations suggested the integration of different coupled semiconductors like Co<sub>3</sub>O<sub>4</sub>/BiVO<sub>4</sub>, CdS/TiO<sub>2</sub>, Bi<sub>2</sub>S<sub>3</sub>/TiO<sub>2</sub>, ZnO/TiO<sub>2</sub>, and ZnO/CuO. Increasing the visible light activity is due to reducing both recombination ratio of the photogenerated electron–hole pairs and compound bandgap (Wang et al. 2005). Several important conditions such as high temperature, complex reactions, time, and the special atmosphere are required for the usual coupling process. However, there are different methods to couple nano-semiconductors by moderate conditions. For example, there is a high feasibility of coupling in moderate conditions by utilizing the ultrasonication process. Viadya et al. integrated titanium dioxide-coated nanoparticles in the shape of a core–shell with ultrasound treatment (Vaidya et al. 2010). Titanium dioxide was utilized

to coat on ZnS and CdS, and the optical properties were remained fixed.

### Nonmetal

By doping with nonmetallic atoms like fluorine, sulfur, boron, phosphorous nitrogen, and carbon, the noticeable enhancement in conventional photocatalysts method has been achieved. Boron can be integrated as interstitial boron where coordination of oxygen and boron is probable or as alternative boron for oxygen, which results in midgap states. Boron on interstitial sites performs as a three-electron donor with the generation of boron ion (III). Nevertheless, both kinds of doping can coexist, which could lead to inner charge transformation. First Zhao et al. (2004) was observed boron-doping, which by sol–gel method and application of boric acid prepared boron-doped titanium dioxide. The energy gap was changed to 2.93 eV by boron doping and was further decreased by acting Ni@B co-doping to 2.85 eV. By visible light irradiation, trichlorophenol was effectively degraded. Singh et al. reported utilizing boron doping with boric acid improved photocatalytic degradation of the organic dyes (Singh et al. 2018).

### Transition metals

Modification with transition metals like Fe, W, Mo, Mn, V, Co, and Cr is one of the major methods of semiconductors activation in the visible area. This method causes the reduction between the conduction gap and valance band. Karan et al. (2010) have studied the doping of transition metals such as Cu or Mn ions in different semiconductor nanocrystals. Bettinelli et al. (2007) investigated the photocatalytic activity of titanium dioxide doped with vanadium and boron on molybdenum degradation, which leads to the increase in molybdenum photodegradation. By visible light, the enhanced photocatalytic activity of BaTiO<sub>3</sub> by Rhodium doping for hydrogen evaluation from the water was observed (Maeda 2014).

### Noble metals

Noble metals loading like Pd, Pt, Au, and Ag on the surface of semiconductors improves the photocatalyst efficiency in dealing with photons, facilitates charge transformation, and hence, slows down the electron–hole pair recombination (Fu et al. 2022). Furthermore, a free-electron can be accumulated at the interface when the metal atoms are excited by light, which is considered as the surface plasmon resonance process (Plodinec et al. 2014). Plasmonic photocatalysis has two crucial properties: localized surface plasmonic resonance (LSPR) and a Schottky junction. The aforesaid properties result in charge transformation and separation, which

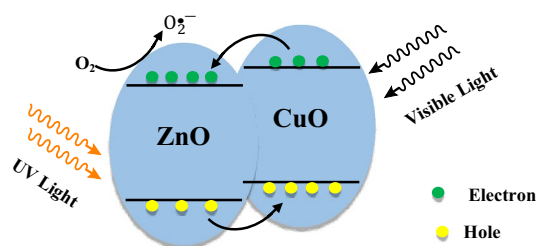


Fig. 2 Doping influence on bandgap (Xu et al. 2017)

promote the excitation of active charge carriers and effective absorption of visible light (Truppi et al. 2019).

## Co-dope

Due to the synergic effects of the co-dope method with double metal or nonmetal dopants or a combination of them for enhancing the visible-light absorption performance of photocatalytic activity, they have been extensively utilized as a promising method. Moreover, it has the potential to prevent the recombination of the photo-induced charge carriers. Table 3 summarizes various co-doped investigations performed by utilizing various elements.

## Catalyst fixation

In the conventional wastewater remediation process, due to the significant surface area, typically photocatalyst nanoparticles are utilized as suspended particles in order to enhance photocatalytic removal efficiency. Employing nanoparticles slurries has inherent disadvantages such as challenging agglomeration of several nanocrystals into large particles, challenges in catalyst reusing, needing a significant quantity of catalysts, expensive liquid/solid separation, and poor settling tendency. Moreover, due to powerful absorptions by dissolved organic compounds and catalysts particles, the extent of ultraviolet light penetration is limited (Herath et al. 2022). One of the ongoing research efforts for improving catalytic efficiency is enhancing a fixed nanocatalyst design with a surface area considerable to that of separate nanoparticles (Jo and Tayade 2016).

Following are the several properties that make utilizing different materials desirable as photocatalyst materials: (1) significant chemical stability; (2) adaptability for application in different kinds of reactors; (3) simple separation from liquid environment; (4) adequate surface adsorption of organic compounds; (5) possessing significant surface area; (6) stable and suitable bonding with catalyst and (7) transmittance toward ultraviolet light. Major beds which can be utilized to immobilize the semiconductors are fiberglass mesh, polymer substrates, silica beads, teflon tubes, porous glasses, and glass by application of chemical vapor deposition, electrochemical manufacturing, sol–gel approach, and thermal fixation (Liu et al. 2022).

## Glass bed

Since glass plates are non-degradable and inactive during the photocatalytic operations and also due to the significant ability of glass for adhering to catalyst powder, compared with other ones, a glass wall or glass bed can be the first option for nano-photocatalysts support. Different kinds of glass have been utilized in catalytic processes like glass tubes and beds, reactor walls, and glass plates (Shah and Patel 2022). The type of photoreactor is one of the significant parameters for determining the type of glass support.

In order to bind the inner glass reactor wall and the photocatalyst particles, a pre-remediation process is required and utilizes a binder which typically is a polymeric binder. To make ZnO on glass plates immobilize, the heat binding approach was employed (Ashour et al. 2022). During this process, a suspension including ZnO in distilled water was used. After making it dry, by using a furnace,

**Table 3** Several investigations related to the co-doped

| Catalyst                         | Degraded Contaminant                 | Dopants                            | References              |
|----------------------------------|--------------------------------------|------------------------------------|-------------------------|
| SrTiO <sub>3</sub>               | NO                                   | N/La                               | Wang et al. (2005)      |
| TiO <sub>2</sub>                 | Toluene                              | N/S                                | Lee et al. (2016)       |
| ZnO                              | Naphthol Blue Black                  | Ce/Ag                              | Subash et al. (2012)    |
| Graphene quantum dots            | Rhodamine B                          | N/S                                | Qu et al. (2013)        |
| g-C <sub>3</sub> N <sub>4</sub>  | Rhodamine B                          | Fe/P                               | Hu et al. (2014)        |
| TiO <sub>2</sub>                 | formaldehyde                         | N/Ni                               | Zhang and Liu (2008)    |
| Bi <sub>2</sub> MoO <sub>6</sub> | Rhodamine B                          | Tb/Eu                              | Li et al. (2017a)       |
| TiO <sub>2</sub>                 | Methylene Blue                       | B/Y                                | Wu et al. (2017)        |
| TiO <sub>2</sub>                 | Diclofenac                           | S–N–C                              | Ramandi et al. (2017)   |
| BiOCl                            | Rhodamine B                          | Yb <sup>3+</sup> /Er <sup>3+</sup> | Yu et al. (2016a)       |
| ZnO                              | Direct red 31                        | In/Sn                              | Bhatia et al. (2017)    |
| CsTaWO <sub>6</sub>              | Water splitting                      | S/N                                | Marschall et al. (2011) |
| BiVO <sub>4</sub>                | methyl orange                        | B/Eu                               | Wang et al. (2013)      |
| InTaO <sub>4</sub>               | Decomposition of an aqueous solution | Mn/Fe/Co/Ni                        | Zou et al. (2002)       |
| TiO <sub>2</sub>                 | Lissamine Green B                    | Cu/Boron                           | Alim et al. (2019)      |



the temperature of the glass plates was increased to 500 °C. During a similar experiment, Sakthivel et al. (2002), by a heat binding approach, supported titanium dioxide nanoparticles onto a glass bed. Titanium dioxide slurry was made with a certain quantity of titanium dioxide in distilled water and, before binding the support, stirred overnight. Then the plate was located in an oven exposed to the temperature of 120 °C. In another experiment (Khalilian et al. 2015), for immobilizing sulfur and nitrogen-codoped titanium dioxide on glass beds, the sol–gel dip-coating method was utilized; after that, the photocatalytic activity was analyzed in a fixed-bed photoreactor.

### Polymer bed

In comparison with ceramic or metal-matrix, polymer-based photocatalyst composites are significantly simple to fabricate. For polymer-based substrate, during decomposition of polymer substrate using active oxygen, a shortcoming is observed (Wu et al. 2021). For application of polymeric substrates, proper solvent and polymer reusability are considered as two crucial parameters. Because of the stable bonding of chemical reactions, it is utilized for providing reusability of both catalyst composite and polymer. Hence, materials which have carboxyl or hydroxyl groups are appropriate for being utilized as substrate.

A practical material that can be employed as photocatalyst support is thermoplastics. Some of their major advantages are possessing significant ultraviolet and chemical resistance, being inexpensive, availability, and not oxidizing. The polystyrene beds are thermoplastic that has a thermo-softening property. Based on the experimental result, an operation including simultaneous removal from water and As (III) oxidation by utilizing immobilized titanium dioxide in PET bottles by thermal treatment in the presence of natural sunlight was studied (Fostier et al. 2008). To immobilization of catalyst for photocatalytic degradation of 4-chlorophenol, Yoon et al. (2011) utilized a polymer-based packed micro-bed reactor. In other investigations (Sarkar et al. 2015), for pharmaceutical wastes degradation, photocatalyst immobilization on a calcium alginate bed was conducted. Moreover, for degradation of organics dyes, immobilizing silver nanoparticles as catalysts on tethered calix hydroquinone was investigated (Mokhtar Mohamed et al. 2015).

### Graphene-dependent beds

In some cases, photocatalysts process are conducted by photo-corrosion which has an adverse impact on catalytic activity. This condition is derived from catalyst solubility in the solution and properties of catalyst bandgap. The aforesaid influence can destroy the photocatalyst structure and decrease the photocatalyst efficiency. In order to overcome

this challenge, some materials like activated carbon, rGO, GO, and CNTs are employed (Mokhtar Mohamed et al. 2015). An easy route including graphene-semiconductor integrated with exfoliated graphene and semiconductor is suspended in a sufficient environment (commonly alcohol, water, or a combination of both), stirred and then dried (Sarkar et al. 2015). Graphene oxide nanoparticles were placed on the carbon electrode, and after that, semiconductor nanoparticles were immobilized on the modified electrode utilizing the solvent evaporation method (Akerdi et al. 2016). By utilizing the hydrothermal approach, zinc oxide particles were immobilized on activated carbon, and their application to eliminate organic dyes was studied (Saini et al. 2017).

### Electrospinning

For the production of a fibrous polymeric composite with a diameter in the nanorange, an efficient novel immobilizing approach known as electrospinning can be utilized. By fiber diameter reduction into lower than micron degree, several properties like increasing the surface area will be remarkably enhanced. The significant surface area is desirable for immobilizing nano-semiconductors as photocatalysts (Heidari et al. 2017). Currently, in order to fabricate semiconductor nanofiber composite by the electrospinning method, an organo-titanium salt coupled with a polymer was utilized, and after that, the composite nanofibers were exposed to a thermal remediation process to obtain the pure semiconductor nanofibers. The particle alignment with improved catalytic property, mesoporosity, and significant surface area are some of the benefits offered by the sol–gel electrospinning-based semiconductor nanofibers. Afeesh et al. (2012) reported a new nematic-formed CdS-doped polyvinyl acetate electrospun mat is established as a reusable and significantly efficacious photocatalyst. The aforesaid nanofiber was able to overcome the challenge of the toxic nature of CdS nanoparticles and photo corrosion phenomena. In order to provide sites for the in situ formation of AgCl crystals, an electrospun cellulose acetate membrane was utilized as support (Zhou et al. 2016). In different studies (Yousef et al. 2012), as easily separable and an effective photocatalyst, CdO/ZnO-doped polyurethane electrospun mat was utilized. By coaxial electrospinning integrated with the sol–gel method, Tong et al. (2014) employed an easy method to direct the spinning of W, Fe, or N doped titanium dioxide nanofibers. By using the sol–gel approach integrated with two capillary spinneret electrospinning methods, long titanium dioxide hollow fibers with mesoporous walls were fabricated (Zhan et al. 2006). Figure 3 demonstrates the SEM images of different immobilized photocatalysts on electrospun fibers.

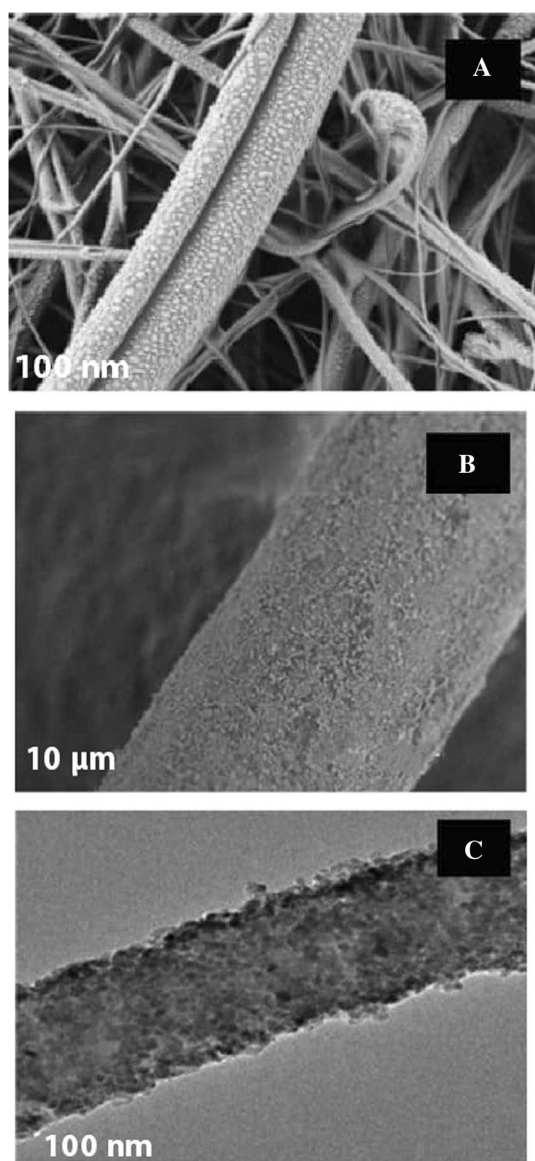


**Fig. 3** SEM image of (a) glass fiber-supported  $\text{TiO}_2$  photocatalyst (Matsuzawa et al. 2008), (b)  $\text{TiO}_2$  particles bonded on a fiber of PES nonwoven (Saini et al. 2017), (c) Au- $\text{TiO}_2$ -loaded electrospun carbon fibers. (Erjavec et al. 2016)

### Magnetic composites

Recyclability of catalyst from treated wastewater would be feasible by magnetizing materials in a photocatalytic composite. As a result, no additional water purification step is required for downstream treatment. The aforementioned method can avoid the catalyst loss over the recovery and also improve the sustainability of the catalyst (De Opereira et al. 2019). By thermal degradation of  $\text{Zn}(\text{acac})_2$  in the reaction environment of preformed magnetite nanoparticles, a novel group of zinc-including magnetic oxides was developed (Aghaeinejad-Meybodi et al. 2021). Zhang et al.

(2013) investigated the synergistic catalytic efficiency of water-soluble magnetic  $\text{g-C}_3\text{N}_4$  photocatalyst and its in situ integration. Metal salt [ $\text{Zn}(\text{CH}_3\text{COO})_2 \cdot 2\text{H}_2\text{O}$  and  $\text{Fe}(\text{acac})_3$ ] were combined with ultrasonically scattered  $\text{g-C}_3\text{N}_4$  sheets in a triethylene glycol mixture. Following the solvothermal reaction, evenly dispersed magnetic  $\text{ZnFe}_2\text{O}_4$  nanoparticles were  $< 10$  nm and effectively placed on the surface of the  $\text{g-C}_3\text{N}_4$  sheet. Xie et al. (2013) integrated a significantly improved photocatalytic activity with a new heterojunction  $\text{SrFe}_{12}\text{O}_{19}/\text{Bi}_2\text{O}_3$  magnetic photocatalyst by utilizing a room temperature sintering approach. In different investigations, immobilization of combined nickel/cobalt metal–organic structure on a magnetic  $\text{BiFeO}_3$  was studied for degradation of water contaminants (Ramezanalizadeh and Manteghi 2017).

### Adsorbents

In order to remove the organic composites and heavy metals during the wastewater treatment process, adsorbents have been utilized extensively (Al-Shalalfeh et al. 2017; Tka et al. 2018). There are different kinds of adsorbents like carbon nanotubes, zinc oxide, polymeric adsorbents, CuO, graphene oxide, zeolite, activated carbon, and silica oxide (Ersan et al. 2015; Wu et al. 2016). Currently, researchers are seeking cost-effective materials which can act as adsorbents like industrial and agricultural wastewater (Hegazi 2013). Orange peels, oil palm shell, neem bark, sugarcane bagasse, coconut, and rice husk are considered examples of inexpensive agricultural side-products (Fernandez et al. 2015). In order to remove the heavy metals from electroplating industries Liu et al., utilized industrial and agricultural wastewater like fly ash and rice husk (Liu et al. 2016). According to the results, fly ash was efficient in the Cu and Cd removal, while rice husk was efficacious in the simultaneous removal of Ni, Pb, and Fe.

It must be mentioned that two adsorbents cannot be compared individually because adsorption efficiency is highly influenced by the adsorbent's properties. Usually, there are minor parameters influencing the adsorption procedure like temperatures and pH value, concentration and adsorbents dosage, inherent properties of adsorbate, and surface area. Table 4 summarizes some essential properties of the adsorbents that have been previously utilized. According to Table 4, it can be detected that oxidized carbon black (OCB) has a high specific surface area, and the investigation was done by Yan-Qing et al. (Yu et al. 2016b) illustrate that the adsorption capacities in the following order: bentonite  $<$  organic bentonite  $<$  CB  $<$  OCB. Nevertheless, the investigation which was done by Rossner et al., revealed that in addition to having an enormous specific surface area, effective adsorbents must have a difference in shape and pore

**Table 4** Attributions of adsorbents

| Adsorbents                        | Zeta potential (mV) | Specific surface area (m <sup>2</sup> ·g <sup>-1</sup> ) | References            |
|-----------------------------------|---------------------|----------------------------------------------------------|-----------------------|
| Zeolite Y                         | –                   | 806                                                      | Rossner et al. (2009) |
| Zeolite Mordenite                 | –                   | 505                                                      | Rossner et al. (2009) |
| MWCNT                             | –                   | 179                                                      | Ersan et al. (2015)   |
| SWCNT                             | –                   | 537                                                      | Ersan et al. (2015)   |
| Graphene oxide                    | –                   | 497                                                      | Ersan et al. (2015)   |
| Montmorillonite                   | –                   | 61                                                       | Macht et al. (2011)   |
| Zeolite X                         | –                   | 0.0844                                                   | Liu et al. (2016)     |
| Al <sub>2</sub> O <sub>3</sub>    | –                   | 168                                                      | Liu et al. (2016)     |
| Ti-Si-O                           | –                   | 181                                                      | Liu et al. (2016)     |
| Ti-Al-O                           | –                   | 433                                                      | Liu et al. (2016)     |
| Oxidized carbon black             | –17.18              | 157                                                      | Yu et al. (2016b)     |
| Carbon black                      | –6.06               | 1114.23                                                  | Yu et al. (2016b)     |
| Bentonite                         | –17.50              | 931.33                                                   | Yu et al. (2016b)     |
| Macronet polymeric adsorbent 500  | –                   | 9.54                                                     | Zhu et al. (2016)     |
| Macronet polymeric adsorbents 200 | –                   | 414                                                      | Zhu et al. (2016)     |
| Synthetic talc                    | –53.560             | 793                                                      | Rahman et al. (2013)  |
| Kaolin                            | –37.324             | 156.91                                                   | Rahman et al. (2013)  |

size and a high pore volume of around 6–9 Å (Rossner et al. 2009). According to their exploration, because of the even shape and size of zeolite pore that makes it only adsorbing pollutants with similar shape and pore size, the carbonaceous adsorbents were more efficient than zeolites.

As shown in Fig. 4, there are various kinds of pollutants adsorption processes, such as the active site of the adsorbent, charge of the adsorbent, and functional groups on the surface of adsorbents. It is obvious that materials that have great quantities of active groups like carboxyl or hydroxyl groups can be utilized to adsorb pollutants with significant removal performance. As a result, different adsorbents were utilized by previous researchers, containing functional groups on the surface of adsorbents (Zhu et al. 2016). They have suggested the application of macronet hyper cross-linked polymeric adsorbents (MN 200 and 500) for pyridine removal from aqueous solutions and detected that because of the presence of non-selective sulfonic acid group on the surface of MN 500; it has a superior adsorption rate (Zhu et al. 2016). The adsorption of water vapor in activated carbon along with functional oxygen groups was explored by

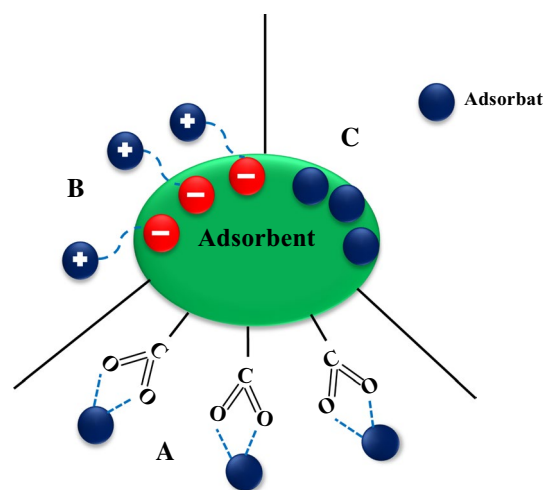


**Fig. 4** Schematic of the adsorption process of pollutants on adsorbents (A) functional groups adsorptions, (B) ion-exchange adsorption, and (C) adsorption ability (Yahya et al. 2018b)

Fletcher et al. (2007). After that, the adsorption mechanism of cupric ions on various kinds of adsorbents like bentonite and organic bentonite, OCB, and carbon black (CB) was investigated by Yu et al. (2016b). The ion exchange adsorption and surface adsorption were two major adsorption mechanisms for carbon black and bentonite. The absorption of oxidized carbon black occurs by the application of oxygen-based functional groups with heavy metal ions, whereas in the case of organic bentonite, it occurs because of the complicated reactions of organic composites in clay interlayer with heavy metal ions.

## Integration of photocatalyst with adsorbents

The combination of photocatalysis and adsorption methods has several attractive advantages for wastewater treatment purposes. Such an integrated approach does not only overcome the significant disadvantages of each method when conducted alone but also maintains all the attractive properties of its components, hence enhancing the total removal performance. Table 5 lists several investigations which have been done for utilizing integrated photocatalyst adsorbents for organic pollutants degradation in the wastewater treatment process. Because of the increasing pollutants adsorption on photocatalyst surface by the adsorbents, many of them reported the enhancement in degradation performance. According to the fact that only a few investigations were conducted on integrated photocatalyst adsorption, still more research attempts are required to determine the potential benefits of this approach for wastewater treatment purposes. Following are various approaches that have been

**Table 5** Previous investigations on integrated photocatalyst adsorption for organic pollutants degradation during the wastewater treatment process

| Catalyst                         | Target material                                                       | Decomposition effectiveness (%) | Adsorbents                            | References                     |
|----------------------------------|-----------------------------------------------------------------------|---------------------------------|---------------------------------------|--------------------------------|
| Ag-AgBr                          | Methylene blue                                                        | 92                              | MMT                                   | Sohrabnezhad et al. (2016)     |
| CoFe <sub>2</sub> O <sub>4</sub> | Cr (VI)                                                               | –                               | Activated carbon                      | Qiu et al. (2016)              |
| C <sub>3</sub> N <sub>4</sub>    | Methylene blue                                                        | 90                              | SiO <sub>2</sub>                      | Zhang et al. (2016a)           |
| Fe <sub>3</sub> O <sub>4</sub>   | Methylene blue                                                        | 100                             | Modified activated carbon             | Xiao et al. (2022)             |
| Ag-CdZnSO                        | Disperse orange 30 dye                                                | 99.5                            | Zeolitic matrix                       | Jaime-Acuña et al. (2016)      |
| BiOBr                            | Rhodamine-B and methylene blue                                        | 98                              | Graphene oxide (GO)                   | Vadivel et al. (2014)          |
| TiO <sub>2</sub>                 | Methyl orange                                                         | 100                             | CNT                                   | Wang and Zhou (2011)           |
| ZnO <sub>2</sub>                 | Methyl orange                                                         | 80                              | Chitosan                              | Kamal et al. (2015)            |
| CuO/Cu <sub>2</sub> O            | 2, 6-dichlorophenol                                                   | 87.5                            | β-cyclodextrin-modified carbon fibers | Chen et al. (2016)             |
| Ag/AgBr                          | Methyl orange and phenol                                              | 95.4                            | Activated carbon                      | Gamage McEvoy and Zhang (2016) |
| CeVO <sub>4</sub>                | Methylene blue                                                        | 98                              | Graphene                              | Fan et al. (2016)              |
| ZnO                              | Rhodamine B                                                           | 100                             | Graphene                              | Bera et al. (2016)             |
| TiO <sub>2</sub>                 | Anions PO <sub>4</sub> <sup>3-</sup> and NO <sub>3</sub> <sup>-</sup> | 100                             | Kaolin                                | Ahmad et al. (2022)            |
| Ag-ZnO                           | Methylene blue, rhodamine B and methyl orange                         | 97.8                            | Graphene                              | Ahmad et al. (2013)            |
| ZnO                              | Methylene blue                                                        | 100                             | Clay                                  | Akkari et al. (2016)           |
| TiO <sub>2</sub> nanotube        | Methylene blue                                                        | 100                             | Carbon-macroscopic monoliths          | Zhang et al. (2016b)           |
| TiO <sub>2</sub>                 | Oxytetracycline (OTC)                                                 | 30.57                           | 5 A Zeolite                           | Zhao et al. (2014)             |
| TiO <sub>2</sub>                 | Phenol                                                                | 90                              | Zeolite (ZSM-5)                       | Torkian et al. (2021)          |
| N-doped TiO <sub>2</sub>         | Tetracycline hydrochloride                                            | 90.2                            | Diatomite                             | Chen and Liu (2016)            |
| Ag-CdZnSO                        | Disperse Orange 30 dye                                                | 99.5                            | Zeolitic matrix                       | Jaime-Acuña et al. (2016)      |
| TiO <sub>2</sub>                 | Dichlorvos                                                            | 89.96                           | Zeolite                               | Gomez et al. (2015)            |
| TiO <sub>2</sub>                 | Amoxicillin                                                           | 88                              | Zeolite                               | Kanakaraju et al. (2015)       |
| Nano-TiO <sub>2</sub>            | Brown-NG (an azo-dye)                                                 | 100                             | Zeolite (ZSM-5)                       | Khatamian et al. (2010)        |

utilized in combination of photocatalyst with adsorbents: wet chemical impregnation (Shaheer et al. 2021), solution process methods (Shaheer et al. 2021), sol–gel (Ahmad et al. 2022), and microwave-based approach (Xiao et al. 2022). The reaction between photocatalyst and adsorbents has a decisive role during the adsorption and degradation performance of integrated photocatalyst adsorbents.

By using a two-step sol–gel approach, Chong et al. (2009) prepared the titania-impregnated kaolinite (TiO<sub>2</sub>/K) photocatalyst. The optimal titania-impregnated kaolinite loading was observed at 6 g/dm<sup>3</sup>, which is equal to 0.48 g/dm<sup>3</sup> of titanium dioxide. According to these outcomes, the annular photocatalytic reactor systems (APR) with the titania-impregnated kaolinite yield higher photo-effectiveness. This is because, in comparison with pure titanium dioxide, the above-mentioned system needs lower titania-impregnated kaolinite loading because of the higher adsorption ability of kaolinite, which increases the feasibility of surface interaction with pollutants. After that, by application of two heterogeneous fluidized bed reactor (FBR) and annular photocatalytic reactor systems, Vimonses et al. (2010) explored

the efficiency of the titania-impregnated kaolinite. Based on their explorations, compared to the APR system, the adsorption of the contaminants by means of the FBR system for eliminating the inorganic nutritious has higher performance, specifically for phosphate. Such results indicate that various processes will have various efficiencies; hence an exhaustive investigation is required for observing proper processes for integrated photocatalyst adsorption in suspended solids.

The previous investigation had suggested a reaction process between targeted material and integrated photocatalyst adsorbents (Nguyen-Phan et al. 2012). Figure 5 demonstrates the suggested photocatalytic degradation reaction mechanism, which occurs in the following order. (a) By the radiation of visible light on photocatalyst, which causes the shifting of an electron from VB to CB, the process is activated. (b) In this condition, graphene oxide as an adsorbent will prevent the recombination of the separated electron meanwhile maintaining them reactive on its surface. (c) The oxidation of OH<sup>-</sup> in water by photo-generated holes, results in the generation of OH<sup>•</sup> (d). The electron keeps on moving across the graphene oxide surface until it interacts



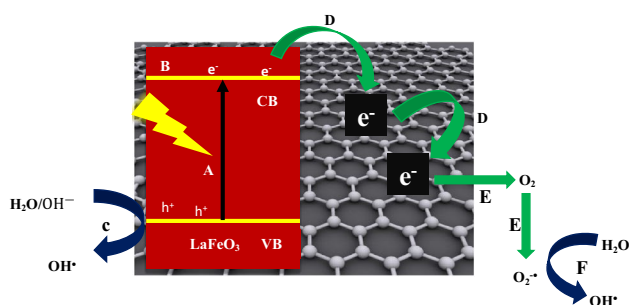


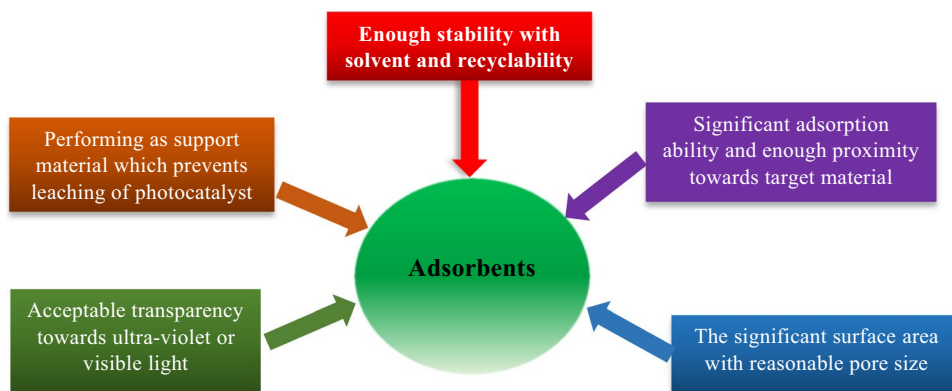
**Fig. 5** Schematic photocatalytic degradation of contaminants using integrated photocatalyst adsorbents (Mutalib et al. 2018)

with the dissolved oxygen. (e) By the reaction between transferring electron and dissolved oxygen  $O_2^-$  is generated. (f) Production of  $OH^\bullet$  is results from the  $O_2^-$ . Degradation of targeted material triggers with the reaction of  $OH^\bullet$  to form a non-toxic compounds. The degradation will be enhanced by adsorbent, which helps concentrate it near the photocatalyst.

### Standards of selection of the adsorbents in integrated photocatalyst adsorbents

As demonstrated in Fig. 6, for selecting the adsorbents as support, some standards must be regarded. (1) Reasonable pore size and significant surface area are essential for the adsorbents. Because it will facilitate high adsorption ability; as a result, increasing the photocatalytic activity (Tafreshi et al. 2017; Taufik and Saleh 2017). Taufik et al. (Taufik and Saleh 2017) integrated ternary mixed oxides on graphene, and the detected surface area of the nanocomposites was increased accordingly photocatalytic activity, and the adsorption ability of the nanocomposite was improved (Taufik and Saleh 2017). (2) For penetrating light toward photocatalyst, adsorbents must be transparent enough toward ultraviolet or visible light. For instance, different graphene-dependent materials are a desirable option for integrated photocatalyst adsorbents processes

**Fig. 6** Selecting standards for the adsorbents in integrated photocatalyst adsorbents processes (Yahya et al. 2018b)



which is because of their inherent properties, including remarkable chemical and electrochemical stability, better electron mobility, significant specific area, and excellent transparency (Vasseghian et al. 2022). For gas cleaning in a fixed bed reactor, granular silica has been utilized by Pucher et al. (2008) as an active adsorbent to coat a porous silica substrate with titanium dioxide-dependent nanoparticles. Because of reasonable ultraviolet transmission of granular silica and significant specific surface area, the final materials show considerable photocatalytic activity and significant adsorption ability during ultraviolet irradiation. (3) To effective distribution of adsorbed substrates to the photocatalytic active sites, the adsorbents should have significant adsorption ability and at the same time have enough proximity to the target material. The ionic strength could be the reason for the proximity between pollutant and adsorbent. Anirudhan et al. (2017) detected that increasing the ionic strength cause reduction of adsorption ability of PAA-g-CGR/TNT composite, which is primarily because of the generation of outer-sphere complexes of the composites with ions. Moreover, it is reported that ions forming inner-sphere complexes demonstrate increasing adsorption ability with increasing ionic strength. (4) The leaching of the metal oxides particles into the treated water must be prevented by application of adsorbents which performs as support material. Since significant numbers of the composites integration include only physical bonding, as a result leaching phenomenon is common (Chkirida et al. 2021). The degree of attractivity between photocatalyst and adsorbents will be determined by leaching. In order to enable the integrated composite to have enough stability with distributed solvent and recyclability, selecting a photocatalyst and adsorbents which are in good harmony is crucial. As it is obvious, for industrial applications, the recyclability of integrated photocatalyst adsorbents will be a significant benefit. Moreover, stable composites will be generated by adsorbents that possess active  $O_2$  functional groups.



## Photocatalyst integrated with graphene

For decades, graphene and its by-products, namely reduced graphene oxide (RGO) and graphene oxide (GO) have been broadly investigated. A single layer sp<sup>2</sup> bonded is the main structure of graphene which makes the fundamental of carbon, CNTs, and fullerenes (Bashir et al. 2021). The unique properties of graphene, including the significant surface area of around 2630 m<sup>2</sup> g<sup>-1</sup> (Alhaddad et al. 2021), excellent mechanical strength, remarkable chemical stability (Li et al. 2021), and proper conductivity, make it one of the attractive materials. After that, the researchers become aware of the advantageous properties demonstrated by graphene for photocatalysis application.

The recombination of electron–hole pairs is considered a critical challenge in the photocatalysis process, which decreases the photocatalytic activity. The integration of semiconductor photocatalyst with graphene as an adsorbent carbon can be performed as an effective carrier for holes and electrons. Wang et al. (2011) have been investigated the ability of graphene as an efficient approach to avoid electron–hole recombination. They revealed photo-induced data between GR and TiO<sub>2</sub> using a temporary photovoltage approach and detected that the meantime was increased from 10<sup>-7</sup> to 10<sup>-5</sup> s when GR integrated with TiO<sub>2</sub> (Wang et al. 2011). Li et al., validated the graphene function in electron transformation by determining the color of the solution (Li et al. 2021). After that, they implemented an experiment on the ZnO with GO suspension to detect the capability of graphene electron transformation. It has been detected that with increasing graphene loading, when the ZnO with GO suspension was radiated with UV light the average lifespan of ZnO emission was reduced from 30 to 14 ns (Kamat 2011).

According to presented investigations, the graphene supported on photocatalyst generated significant photocatalytic efficiency primarily because of the composite light absorptivity and improvement in the adsorption ratio of contaminants (Yahya et al. 2018a). Moreover, graphene can perform as a sensitizer to enhance the performance of integrated photocatalyst adsorption against light radiation and increasing efficiency of the photocatalytic activity. As one of the graphene by-products, graphene oxide has proper quality material for supported photocatalyst because it includes an extensive range of non-selective oxygen functional groups like hydroxyl, epoxy, and carbonyl groups on the surface. As a result, graphene oxide can interact with an extensive range of molecules and hence can experience surface modification (Lightcap et al. 2010).

Catalyst loading is considered one of the major parameters that have been demonstrated to have considerable impacts on improving photocatalytic activity. Catalyst loading can increase the photocatalytic activity and hence, increase the performance of contaminants degradation.

However, increasing catalyst loading until a particular threshold could decrease photocatalytic activity by improving absorption and scattering of photons by extra carbon which presents in the composite (Singh et al. 2018). As a result, graphene loading contents perform critically in determining photocatalytic activity of composite.

## Photocatalyst integrated with zeolite

Zeolites are hydrated aluminosilicate minerals, including oxygen, silicon, and aluminum, in their structure. In terms of composition, they are identical to clay minerals; nevertheless, the crystalline framework of zeolite is different. Because of its significant surface area, charged structure with amphoteric properties and considerable adsorption ability of zeolite is regarded as essential adsorbents. Moreover, its special Al-O units which can decrease the electron–hole recombination rate, rendering it an attractive option for integrated photocatalyst adsorbents applications (Torkian et al. 2021).

Kanakaraju et al. (2015) considered that the degradation of amoxicillin using incomplete hydrolysis is due to the acidic feature of the zeolite and titanium dioxide (Kanakaraju et al. 2015). Zhao et al. (2014) have various ideas regarding the adsorption process of pollutants on adsorbents. They suggested that electrostatic attractions are the reason for the adsorption of organic compounds on adsorbents, and according to their investigations, at higher values of pH (greater than 11), electrostatic repellent decreased adsorption to the least possible amount. Moreover, because of the hydrophobic feature of zeolite, presence of it as an adsorbent improves the photodegradation of contaminants. According to the experimental investigations of Takeuchi et al., significant hydrophobic properties of zeolites cause increasing photocatalytic oxidation of gaseous acetaldehyde (Takeuchi et al. 2009). As a result, designing a properly integrated photocatalyst adsorption system for special pollutants can be performed by selecting a suitable adsorbent with special properties.

## Photocatalyst integrated with activated carbon

From the combustion of carbonaceous materials like plant-dependent or coal, activated carbon (AC) is produced (Saleh 2018). Typically, the production of activated carbon includes the activation and carbonation process. The application of activated carbon as the absorbent and support for the photocatalyst process has been employed for different kinds of composites such as Ce/AC (Sharma et al. 2019), ZnO/AC (Jonidi Jafari et al. 2021), Ag/AgCl/AC (Liu et al. 2016), and doped TiO<sub>2</sub>/AC (Huang et al. 2011). Mainly, the presence of activated carbon increases the contact between contaminants

and photocatalyst; as a result, increasing the degradation rate by absorption process.

The presence of organic pollutants has been a significant challenge. Photocatalysis technology is shown much promise for the degradation of organic pollutants in different wastewaters, alongside titanium dioxide as the photocatalyst, which possessed outstanding properties such as activation by ultraviolet irradiation, cost-effectiveness, non-toxicity, and chemical stability (Choi et al. 2006). Moreover, to modify the properties of titanium dioxide versus visible light, its doping is investigated extensively. It is well-established that the synergistic effect of activated carbon with titanium dioxide is enhancing the photodegradation ratio of different contaminants (Tryba 2008). In order to improve N-doped titanium dioxide coated on activated carbon, Huang et al. (2011) have integrated the vapor hydrolysis and impregnation methods (Huang et al. 2011). Form with grain size varying from 10 to 20 nm, the visible light-induced photocatalyst was generated in anatase. It was reported that while the active surface of AC could be damaged by preventing titanium dioxide, the distribution of titanium dioxide into AC could improve the photocatalytic activity (Pang et al. 2020). As an approach for the degradation of toluene during ultraviolet irradiation, the sol–gel Zn<sup>2+</sup>-TiO<sub>2</sub>/AC composite was effectively fabricated (Ali et al. 2020). It was reported that in comparison to pristine TiO<sub>2</sub>/AC photocatalyst, the photocatalyst activity was increased because of the doping of Zn<sup>2+</sup>. However, it was detected that 20% zinc doping was the optimum loading because the significant band-gap energy of zinc would block the light absorption of titanium dioxide. Moreover, in comparison with pristine titanium dioxide, the resultant photocatalyst has maintained higher photocatalytic degradation performance.

### Photocatalyst integrated with clays

Because of the cost-effective and earth-abundant feature of clay minerals and different clay-based materials, application of them is quite advantageous. They can be categorized into four groups which include chlorite, illite, montmorillonite-smectite, and kaolinite. They present porous heterostructures that converted them from inactive materials to highly activated materials in the adsorption process. Moreover, because of their significant cation transfer potential, phyllosilicates material, physical and chemical stability, and broad surface area, they have been known as effective adsorbents (Zou et al. 2022).

Thanks to its excellent structural features and different unique properties, including its extensive application as adsorbents combined with another photocatalyst, they had absorbed significant focus in wastewater treatment processes. The influence of ZnO in nano-ZnO/bentonite was explained by previous investigations (Xu et al. 2015). According to the

outcomes, with using ZnO content varying from 10 to 60%, the photocatalytic activity was increased and then reduced once ZnO content had reached 70%. Because ZnO had controlled the hybrid, an additional quantity of it had avoided bentonite to perform effectively. When titanium dioxide was supported on palygorskite clay mineral, a higher rate of orange G degradation was obtained (Bouna et al. 2013). Because excessive photons due to the significant surface area shown by titanium dioxide-palygorskite, in concentrations less than the optimal ones, complete radiation toward the surface of a particle was obtained (Bouna et al. 2013).

### Influential factors in the photocatalytic process

Several crucial factors are considerably controlled the rate constant and the degradation performance of the photocatalyst process. Different influential and operational parameters that demonstrated substantial effects on the photocatalytic mechanism are briefly explored following.

#### Solution pH

The process of adsorption, which is the first step of photocatalytic removal, considerably depends on the pH value. By influencing the value of electrical charge and deprotonation of surface functional groups, various kinds of degradation products were generated. Moreover, the pH of the solution significantly affects the photocatalytic dye degradation and the dye adsorption into the semiconductor surface as a catalyst surface. At pH great values of pH or neutral, OH<sup>•</sup> primarily performs as an oxidation factor, and at lower ones, a positive hole performs as an oxidation factor. Hence by changing the value of pH, the system efficiency will improve substantially.

Sometimes, the most significant value of the degradation rate is detected. The point of the zero charges of the photocatalyst is the reason for these results. Understanding this point makes us regulate the absorption or repellent of catalysts-organics electrostatically. In Jallouli et al. research, the pH of 5 and 4.5 was recommended as optimum points for the degradation of ibuprofen and phenol, respectively (Jallouli et al. 2018). At pH 5 and 4.5, based on the point of zero charges of their photocatalyst (titanium dioxide almost 6.6), the phenol and ibuprofen molecules are negatively charged, whereas the titanium dioxide surface is positive. The highest electrostatic reaction between the photocatalyst and contaminant causes the minimum degradation rate. The outcomes demonstrated that borate addition in mixture and loading of Pt in TiO<sub>2</sub> could significantly influence the hydrogen peroxide generation and degradation. The hydrogen peroxide degradation leads to the OH radicals formation. The highest

borate adsorption on titanium dioxide was observed at pH 9.0. Adding borate increased the quantity of hydrogen peroxide generation of Pt/TiO<sub>2</sub>. Also, fluorescence calculation at pH 9 demonstrated the highest intensity for borate integrated with Pt/TiO<sub>2</sub>, which accordingly caused the highest degradation rate of phenol at that pH. Moreover, it was detected that pH has no impact on the degradation performance of dinitrotoluenes and nitrotoluenes (Kumar and Davis 1997). This event is because of the absence of any pH-based difference in nitrotoluene proton accepting or donating over the pH ranging from 3 to 11.

During the photocatalytic process, the amount of pH is a crucial factor in determining the properties of both solute molecules and solid catalysts (Rostami et al. 2019). In order to degrade the organic compounds in water by photocatalyst method, the pH has different influences at different steps: (a) generation of OH<sup>•</sup>, (b) accumulation of photocatalyst particles, (c) the photocatalyst VB and CB position, and (d) ionization state of photocatalyst surface (Hekmatshoar et al. 2020).

By reducing the pH value, the photocatalytic degradation performance of 4-NP will be increased. The highest amounts of photo-degradation were detected in significantly acidic conditions. These results are in good harmony with the results suggested by Shokri (2021).

Because pH can change both charges of the catalyst and pollutants, the amount of pH is an essential parameter in the photocatalytic process. Hence, its initial value was set into 3, 7, and 11. The changing of the substrate surface could be the main reason for the influence of pH, which would further influence the pre-adsorption process. The separation of 4-Nonylphenol was different at different values of pH. Moreover, the surface charge of catalysts was related to their points of zero charge. Also, the oxidation energy of OH<sup>•</sup> and the Fermi level of the photocatalyst was reported to be influenced by different values of the pH in order to degrade contaminants by photocatalyst. As a result, in the alkaline environment, the electrostatic reaction between 4-Nonylphenol and catalysts was remarkably limited (Schneider et al. 2014). The response value was affected by the value of pH, and the maximum degradation rate was obtained at pH 3. Furthermore, the previous investigation of researchers suggested the same outcomes, that the degradation of anionic compounds is more in acidic environments. It is due to the fact that the catalyst surface becomes negatively charged if the pH value goes beyond the ZPC of titanium dioxide; hence adsorption will be lower (Shokri and Mahanpoor 2018).

### Photocatalyst dosage

An optimized concentration of required photocatalyst is determined based on the reactor volume, contaminant size, and different kinds of photocatalyst to enhance

photocatalytic removal efficiency. In several investigations, an optimized point for photocatalyst quantity was suggested. Such outcomes were achieved from the observations that (1) increasing opacity and light emission of ZnO are occurring at significant concentrations, and (2) photocatalyst particles agglomeration occurs at significant concentrations, reducing the number of surface active sites (Jallouli et al. 2018).

The concentration of the catalyst considerably influences photocatalytic activity. Also, its value is directly correlated to the catalyst loading in a heterogeneous photocatalyst. Due to undesirable light emission and decreasing light penetration into the solution because of excessive loading of the photocatalyst, the photodegradation rate increases with increases in the quantity of photocatalyst and after that reduces with increasing catalyst concentration. To prevent further catalysts usage, it is essential to determine the optimal loading of the catalyst for effective pollutant removal. Nevertheless, the required catalyst quantity is based on particle morphologies, the intensity of light, and the reactor design. As a result, incompatible catalyst loading has been investigated in different research (Pourfalahoon et al. 2021).

### Direct photolysis process

Ultraviolet light bulbs, which are utilized in photocatalytic reactors, typically have a wavelength of 254 nm with a relative significant photoelectric conversion performance. Such low-pressure mercury light bulbs have the potential for a generation of mercury resonance lines at 185 and 254 nm. Depending on the ultraviolet light bulb energy and its producer, the efficiency of the light bulbs with 185 nm wavelength changes from 8 to 25% (Zoschke et al. 2014).

An easy method for the photocatalytic degradation of organic contaminants is the direct photolysis process. In comparison with the reaction without utilizing a catalyst, a usual photolysis reaction that is carried out with a photocatalyst process demonstrates considerable efficiency. Solar simulators, ultraviolet or xenon light bulbs, can be utilized in the process. The photolysis process is influenced by different parameters like the pH value and the concentration of organic contaminants (Truppi et al. 2019).

### Photocatalyst nature

The photocatalytic activity of various photocatalysts is different according to impurities on the catalyst surface, particle size, surface area, morphology, and lattice structure. All aforementioned factors considerably influence the rate of electron–hole recombination, electron life span, and the adsorption nature of the organic materials on the catalyst surface (Bie et al. 2021). One of the broadly utilized photocatalysts is considered titanium dioxide. Titanium dioxide has three various phases: brookite, rutile, and anatase

with various lattice designs. Nevertheless, the anatase  $\text{TiO}_2$  is more effective for photocatalytic activity since surface peroxide groups with significant stability can be formed in anatase. Currently, it has been suggested that in comparison with the single-phase rutile and anatase, the combined phase of them can perform effectively. Also, the active sites for the reaction and the surface area on the catalyst are directly proportional, which is directly related to degradation performance. Higher active sites will yield higher adsorption for degradation and, as a result, advance the degradation efficiency.

### Radiation time and intensity of the light

The photocatalytic activity rate is based on the photon absorption and the amounts of photons falling on the surface of the catalyst. At low light intensities ( $0\text{--}20\text{ mW cm}^{-2}$ ), recombination is minor and electron–hole formation is considerable. In this situation, by increasing light intensity, the rate constant increases linearly. With increasing light intensity around  $25\text{ mW cm}^{-2}$ , electron–hole separation is challenging with recombination, which reducing the light intensity influence at a rate constant. Nevertheless, the reaction rate is reversely proportional to the radiation period since the photocatalytic degradation of the pollutants follows the pseudo-first-order kinetics. Hence, after the optimal period, the reaction ratio reduces, which is primarily attributed to the catalyst deactivation because of the strong deposition of the side-product.

### Dissolved oxygen

In order to decrease the recombination and trapping the electrons from the CB, dissolved oxygen in the solution performs as an electron scavenger. Hence, with increasing in dissolved oxygen, photodegradation will increase. The ratio of electron transformation from the catalyst surface to dissolved oxygen will be significantly increased if the quantity of dissolved oxygen is higher in comparison with the electrons which produced by photocatalytic activity at the surface. Moreover, dissolved oxygen has contributed to the stabilizing process of direct photocatalytic reactions, mineralization, and radical intermediates (Gao et al. 2021).

### Initial pollutant concentration

The adsorption of pollutants on the catalyst surface, which is mainly based upon the initial concentration of pollutants, significantly influences the effective photocatalyst activity. As a result, the photodegradation mechanism highly depends on the initial pollutants concentrations. In this condition, the pollutants ions will cover more active sites, and lower photons can come to the surface. Hence, a lower quantity

of hydroxyl radical will be produced. So, the operation can be prevented by the higher pollutant concentrations, which reducing degradation performance (Kumar 2017).

### Temperature of the reaction

The rate constant of the photocatalytic activity is remarkably influenced by the temperature of the reaction. Arrhenius equation is utilized to describe it, for which the evident first-order rate constant must increase linearly with  $\exp(-1/T)$ . Hence, by increasing the temperature up to  $80\text{ }^\circ\text{C}$ , the rate constant increases. Due to the recombination losses of carriers and negligible adsorption of organic materials on the surface of titanium dioxide, the rate constant of the reaction reduces for temperatures above  $80\text{ }^\circ\text{C}$ . As a result, a reaction temperature below  $80\text{ }^\circ\text{C}$  is beneficial for an effective photocatalytic degradation. Nevertheless, the activation energy will be increased if the temperature decreases to  $0\text{ }^\circ\text{C}$ . So there is an optimal temperature range for photocatalytic activity to reach an effective quantity of degradation (Gnanaprakasam et al. 2015).

### Influences of adding oxidizing groups

By addition of different powerful oxidizing groups like potassium peroxydisulfate ( $\text{K}_2\text{S}_2\text{O}_8$ ),  $\text{KBrO}_3$ ,  $(\text{NH}_4)_2\text{S}_2\text{O}_8$ , and hydrogen peroxide to titanium dioxide suspensions, the electron–hole recombination effect can be reduced. Since hydrogen peroxide increases the hydroxyl radical quantity, in most of the photocatalytic processes, hydrogen peroxide is utilized as an additive factor during two following processes: (1) self-degradation during irradiation and (2) accepting an electron from the conduction band results in hydrogen peroxide reduction to hydroxyl radicals on the catalyst surface and hence, facilitating charge separation. By reducing the electron–hole recombination and increasing the hydroxyl radicals at low concentrations, hydrogen peroxide increases the component's degradation. Nevertheless, at hydrogen peroxide concentration higher than the critical concentration, the electron acceptors react with  $\text{TiO}_2$  or with the hydroxyl radical and perform as a hydroxyl scavenger or hole to produce peroxy compounds, which decreases the photocatalytic activity (Zheng et al. 2021).

### Influence of inorganic salts

The pollutants in wastewater can be significantly influenced by different inorganic anions and ions which exist in it. Inorganic anions like sulfates, nitrate, chlorides, and carbonates and cations like zinc, magnesium, calcium, iron, phosphate, and copper present in the different wastewaters. Due to their highest oxidation state, cations like zinc, magnesium, and calcium demonstrate negligible influence on the activity.



However, cations like iron, phosphate, and copper have demonstrated a significant reduction in the photodegradation process performance since such cations coat the active sites on the surface of titanium dioxide and cause catalyst deactivation, which decreasing the photocatalytic activity. Moreover, the presence of anionic salts reduces the surface contact between the photocatalyst and target dye molecule, increases mass transformation rate, and colloidal instability, which decreases the degradation of the pollutants. The reduction in degradation performance in the presence of  $\text{Cl}^-$  is because of their hole scavenging properties. Also, the catalyst surface can be blocked by the presence of chloride ions (Zafar et al. 2021).

## Assessing effectiveness of photocatalyst process

The efficiency of semiconductor photocatalyst is evaluated by various factors like photonic effectiveness, first-order rate constant, and degradation performance. Quantum efficiency and turnover number are two other factors that are utilized to investigate the efficiency of photocatalytic hydrogen evaluation reactions. However, the aforesaid efficiency-determine factors are based on various cumulative factors of the reactor design. Hence, the catalyst efficiency will be different for various types of organic contaminants, reactors, and catalysts.

### Degradation effectiveness

To calculate the performance of the catalyst over the photocatalytic reactions, the concentration of target degraded contaminants in the liquid phase is crucial. In this way, the following equation is used:

$$\text{Degradation effectiveness} = \left(1 - \frac{C}{C_0}\right) \times 100\% \quad (6)$$

where  $C$  is the concentration after a certain radiation period, and  $C_0$  is the pollutant concentration prior to irradiation (Miao et al. 2021). Beer-Lambert's rule under the equation of  $A = \epsilon cd$  is utilized to measure the concentration of the organic material in the liquid phase where  $c$  is the absorber concentration of the absorbing particles,  $\epsilon$  is the molar extinction coefficient, and  $A$  is the absorbance.

### Photonic effectiveness

Photonic effectiveness is known as the number of reactant molecules, which is transferred or generated divided by the number of photons at a given wavelength on the reactor cell. Moreover, the photonic effectiveness might be determined

by the correlation of the initial ratio of substrate degradation to the amounts of photons coming to the reactor as measured by the actinometry. The photonic effectiveness is characterized as  $\mathcal{L} = R_{\text{in}}/R_{\text{o},\lambda}$  where  $R_{\text{o},\lambda}$  is photon flow, and  $R_{\text{in}}$  is the initial rate constant. In order to prevent inessential mistakes considering the reactor geometry, surface area, and size of the utilized photocatalyst and light source, the relative photonic effectiveness could be employed to compare experiments with a similar laboratory or with other ones (Ferreira et al. 2021). The relative photonic effectiveness will be independent reactor factor, and it is described as:

$$\mathcal{L}_r = \frac{R_{\text{in}}(\text{Substrate})}{R_{\text{in}}(\text{Organic molecule})} \quad (7)$$

$$\text{w h e r e } R_{\text{in}}(\text{substrate}) = \frac{R_{\text{in}}(\text{substrate})}{R_{\text{o},\lambda}} \quad \text{a n d} \\ R_{\text{in}}(\text{Organic molecule}) = \frac{R_{\text{in}}(\text{Organic molecule})}{R_{\text{o},\lambda}}$$

### Quantum efficiency

To compare the photocatalytic activity of various photocatalysts, experimental conditions like concentration, light source, and reactor design must be constant. However, in operational conditions, governing all the experimental conditions is challenging. In order to prevent the experimental conditions in the effectiveness parameter, the quantum efficiency is utilized. Typically, the number of the incident to absorbed photons on the catalyst surface is explained as quantum effectiveness. Utilizing Si photodiode or thermopile, the number of the incident photon can be calculated. However, due to light emission, it is hard to calculate the number of photons absorbed on the surface. In such conditions, the evident quantum effectiveness is measured, and it is lower compared to the actual quantum efficiency. Evident quantum effectiveness can be explained by the rate of reaction to rate of incident radiation (Eq. 8) (Navakoteswara Rao et al. 2021).

$$\text{Quantum efficiency } (\Phi) = \frac{\text{Number of reacted electrons}}{\text{Number of incident photons}} \quad (8)$$

### Rate constant

The Langmuir–Hinshelwood (L–H) model is utilized for the assessment of photocatalytic reaction efficiency, which is happening in the liquid–solid medium. The temperature, intensity of light, contaminant concentration, and reaction elements can be integrated using the aforesaid model (Shokri et al. 2017). The Langmuir–Hinshelwood equation in photocatalytic process can be simplified as the following:



$$-\frac{dC}{dt} = kC \quad (9)$$

where  $t$  is the respective period,  $k$  is the rate constant, and  $c$  is the concentration. Using the following equation, the rate constant can be measured:

$$-\ln\left(\frac{C}{C_0}\right) = kt \quad (10)$$

where  $k$  is the first-order constant rate measured by the slope of  $\ln C_0/C$  versus  $t$  slope,  $C$  is the concentration after the reaction, and  $C_0$  is the initial concentration.

### Turnover number

The turnover number is utilized in the photocatalytic hydrogen evaluation reaction to determine the photocatalytic reaction without any other secondary reactions. In comparison with a photocatalyst, the amount of  $O_2$  and  $H_2$  must be higher. Otherwise, secondary reactions might be happening. Turnover number is explained as:

$$\text{TON} = \frac{\text{Number of reacted molecules}}{\text{Number of active sites}} \quad (11)$$

However, it is hard to measure the number of active sites in a photocatalyst. As a result, the turnover number can explain the number of reacted electrons to the number of atoms in the photocatalyst or its surface.

$$\text{TON} = \frac{\text{Number of reacted electrons}}{\text{Number of atoms on the surface}} \quad (12)$$

From the number of  $H_2$  the number of reacted electrons can be measured. Nevertheless, since the number of atoms on the surface is more than active sites, the measured turnover number is smaller compared with the measured turnover number by utilizing active sites (Rajbongshi 2020).

### Challenges in photocatalyst process

As discussed previously, because of the outstanding properties of semiconductor metal oxides like ZnO and  $TiO_2$ , they advent as a promising and effective photocatalyst for use in the wastewater treatment. Some of those attractive properties include application in fuel production, disinfection, detoxification, lower toxicity, higher stability, and broad bandgap. Moreover, assorted morphologies, higher surface states, and significant surface area can be provided by using different types of nanomaterials, which is beneficial for solar photocatalytic reactions. However, because of the several serious problems concerned with the semiconductor metal oxides, the performance of the

solar photocatalyst is still low. The main challenges in the photocatalyst are briefly discussed here.

### Spectral discrepancy

The bandgap energy ascertains the absorption of the incoming photon and, as a result, the photocatalysis performance is regarded as the photocatalyst first challenge. The solar spectrum includes 55% IR, 40% visible light, and 5% ultraviolet wavelength. Whereas a main portion of the solar spectrum is within the visible wavelength, the significant numbers of the semiconductors have significant bandgap value, which can absorb simply the ultraviolet section of the solar spectrum. Hence, modification of the bandgap of the semiconductor photocatalysts is a significant challenge that must be overcome as the prime concern.

### Recombination of photo-generated charges

The recombination of holes and photogenerated electrons is regarded as significant challenge that remarkably affects the photocatalytic activity of a semiconductor. After the formation of electron-holes they transfer to the surface for reduction and oxidation. Over the transferring, recombination of photogenerated charge carriers might occur either on the surface or in bulk by dissipating the energy as heat or light, hence limiting the photocatalytic activity. For the separation and transportation of charges, energy shortage causes a tiny portion of charge carriers to be separated and contributed during the reactions, while, because of nonproductive recombination, a significant number of the charge carriers are lost. By defects or impurities in the crystal, the recombination process is improved. As a result, to improve photocatalyst activity, decreasing the recombination is significantly crucial (Cheng et al. 2014).

### Low surface area

Since the surface power plays a pivotal role in the electron transformation between the reactant in the photocatalyst process, the photocatalysis activity is affected by the interface/surface chemistry. The catalytic reaction in a heterogeneous catalyst occurs at the interface or surface. Hence, the catalyst specific surface area is one significant parameter that determines the process effectiveness; the higher photocatalytic activity, the higher the specific surface area (Cheng et al. 2014).

## Some techniques for improving photocatalytic activity

As demonstrated in Fig. 7, for improving the photocatalysis activity of a semiconductor photocatalyst by solar/visible irradiation, various approaches have been utilized. The semiconductor bandgap should be modified based on the solar spectrum in order to effectively harness solar energy. Band structure modification is the most efficacious approach to modifying the bandgap. As shown in Fig. 7, various approaches have been suggested for a band structure modification. If both surface and bulk recombination of the charges decrease, the efficient usage of produced photons can be feasible. In order to control this recombination, the utilized methods are the reduction and oxidation reactions based on the surface active sites, integration of electron scavengers, and metal oxide heterojunction. As a result, the surface design and morphology play a pivotal role in the photocatalysis process.

## Modulation of designing electronic band for sunlight harnessing

Modification of the conduction band and valence band in the semiconductor is one way to improve photon harnessing. By adding different impurities to the structure of a single semiconductor, the modulation of its band is feasible. They can provide localized electronic states between the conduction band and valence band, which decrease the bandgap, and as a result, based on the element properties and level of doping, light absorption wavelength is shifted to the visible area. Moreover, by generating a homo-junction interface of the semiconductor with a regulated integration approach, modulation of band structure for light harnessing in a single semiconductor is feasible.

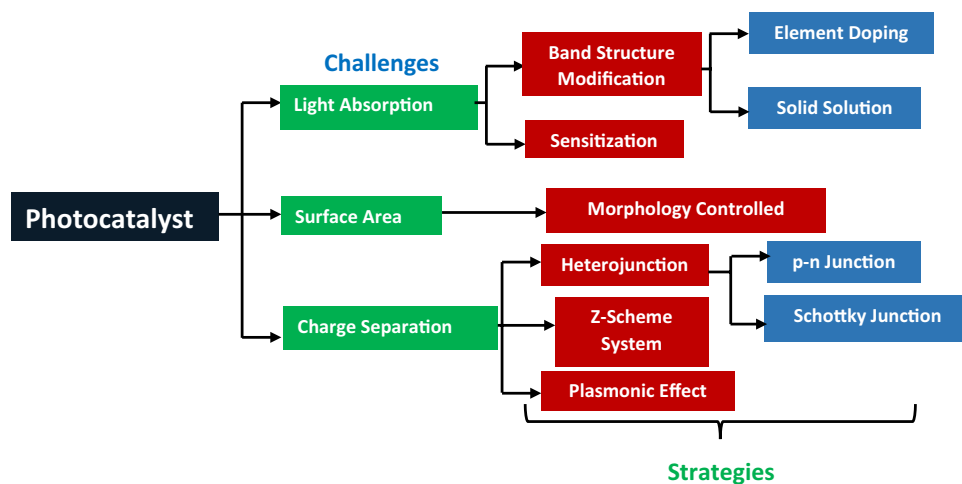
## Photocatalysts with single semiconductor

During the photocatalyst process, charge separation is a significantly essential and complex parameter, and it has a pivotal role in photocatalysis activities. Since semiconductors usually have different phase designs to form phase junctions in controlled synthesis conditions, increasing the charge separation in the photocatalytic phase junction is a broadly utilized method. The commercial  $\text{TiO}_2$  photocatalyst, Degussa P25, which has an anatase–rutile mixed-phase design, is considered as a standard titanium dioxide for its significant photocatalysis activity. The synergistic effect between rutile and anatase is the reason for the perfect efficiency of P25. All  $\text{TiO}_2$  polymorphs demonstrate various light absorption properties based on their bandgap and have various crystal designs. By improving charge separation and light absorption, the production of mixed-phase homo-junction of the semiconductor can improve photocatalysis activity. Integrating two various polymorphs causes changes in the individual polymorph bandgaps, and as a result, the total bandgap of photocatalyst decreases. The bandgap of rutile and anatase is 3.03 eV and 3.2 eV, respectively. Nevertheless, their mixed phase titanium dioxide demonstrates the bandgap between 3.03 and 3.2 eV (Chen et al. 2021).

## Constantly tuning band design by solid solutions

Another effective method to sensitize the photocatalyst for the visible, active area is tuning the CB and VB. Hence, the solid-solution photocatalysts production with constant bandgaps advent as a prerequisite for visible, active photocatalysts. Different kinds of energy band manipulations limit the redox potential. As a result, striking a proper balance between sufficient redox potentials and efficient visible light absorption is essential. Hence, the solid solution photocatalysts production with constant bandgaps is the focus of attention. For constant manipulations of the bandgaps, the

**Fig. 7** Various methods and challenges for an efficacious photocatalyst process (Rajbongshi 2020)



constant modification of the CB and VB or both methods simultaneously have been investigated.

### Engineering of energy band

By changing the light absorption property and determining the redox potential, the engineering of the energy band of a semiconductor photocatalyst has a pivotal role in improving photocatalysis activity. Engineering of the energy band is an efficient method for the improvement in visible, active photocatalysts with enhanced performance to the efficient application of the solar spectrum in a photocatalytic process. For bandgap engineering, three methods have been suggested: (1) constant modification of the conduction band or valence band, (2) metal doping or the conduction band modification, and (3) nonmetal doping or valence band modification.

### Heterogeneous designs for improved charge separation

In order to overcome the challenges in the photocatalytic process, fabrication of heterojunction with noble metals and different semiconductor oxides is broadly utilized. Heterojunction can demonstrate different advantages: (1) photocatalyst stability enhancement because of the suitable surface passivation, which protects the surface for side-reaction and direct electrochemical reaction that may result in catalyst degradation; (2) the photocatalyst stability, efficient charge separation, and optical absorption; (3) the Schottky junction (semiconductor/metal) and semiconductor/semiconductor (p-n junction), which leads to effective charge separation; and (4) sensitizing the materials with a high bandgap, results in light absorption improvement.

### Sensitization

Photocatalyst sensitization is another broadly investigated method for visible, active photocatalyst. The molecular structures are utilized in order to modification of the semiconductor surface. In the photocatalytic process, various nonmetal and complicated metal dyes have been improved and employed to sensitize semiconductor photocatalysts with a broad bandgap. Figure 8 demonstrates the fundamental process of the dye-sensitized photocatalyst. According to Fig. 8, during light radiation, the photoexcited electrons move from the highest occupied molecular orbital level to the lowest unoccupied ones. The excited electrons transfer into the conduction band of the semiconductor, which occurs in the reactions, and dyes remain as cationic radicals. For contaminants in the wastewater, various dye-sensitized photocatalysts have been reported (Reddy et al. 2016). Moreover, currently quantum dot

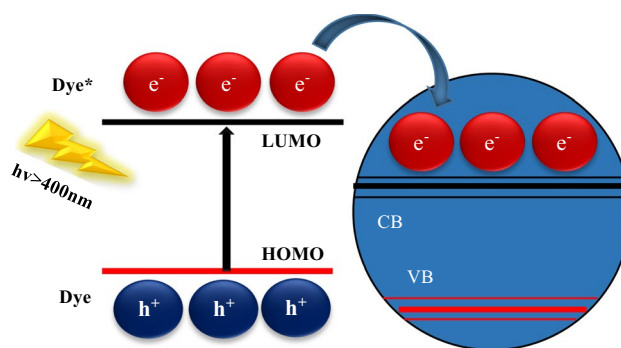
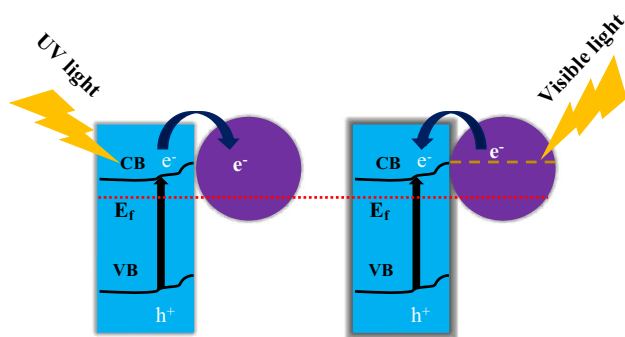


Fig. 8 Dye sensitization-based photocatalyst (Rajbongshi 2020)

(QD)-sensitized photocatalyst has been utilized for the degradation of organic pollution. Quantum dots are nanoscale around 2–10 nm particles which demonstrate different benefits: (1) significant surface-to-volume rate, (2) generation of different charge carriers plus a single high-energy photon, and (3) the customized bandgap for being in visible region. In visible light, a quantum dot can produce electrons that are transferred into the semiconductor conduction band. Nevertheless, for effective electrons transformation from the quantum dot to the semiconductor conduction band, the CB edge of the quantum dot should be over that of semiconductor materials (Reddy et al. 2016).

### Charge transfer and surface Plasmon resonance mediated light absorption

By two various procedures in the photocatalytic process, charge transfer and light absorption can be improved by different kinds of metal-based nanoparticles, (a) showing optical excitation and generating a consistent fluctuation of the free electrons which can generate resonance with incoming electromagnetic radiation and (b) trapping freely emitting light in the semiconductor. The aforesaid mechanism is considered as local surface plasmon resonance. The local surface plasmon resonance influence of different metal-based nanostructures can improve the absorption in various wavelengths and hence increase the photocatalysis activity of the nearby semiconductor. The function of metal-based nanoparticles for improving photocatalysis activity is various based on the incident light wavelength. In the visible light radiation, because of the local surface plasmon resonance influence, metallic nanoparticles can produce several hot electrons which are transferred to the conduction band of the semiconductor for additional reactions, however in ultraviolet light, they can entrap the electrons from the CB of the semiconductor (see Fig. 9) (Wu 2018).



**Fig. 9** Surface plasmon resonance influence on a photocatalyst at various wavelengths (Rajbongshi 2020)

### Semiconductor Schottky junction

In photocatalytic activity, metal nanoparticle loading on the photocatalyst surface plays a pivotal function. Different noble metals like Pd, Au, Pt, and Ag have been explored in the photocatalytic process. A Schottky junction can be created between the semiconductor and the metal nanoparticle by noble metals loading on a photocatalyst. According to Fig. 10, in Schottky junction, Fermi level alignment between the semiconductor and metal generates a built-in electric field in the space-charge area close enough to the interface, which can improve the separation of the photogenerated holes and electrons. Moreover, metallic nanoparticles can perform as a catalyst which decreases the gas evolution procedures or the potential for surface electrochemical reactions (Huang et al. 2021).

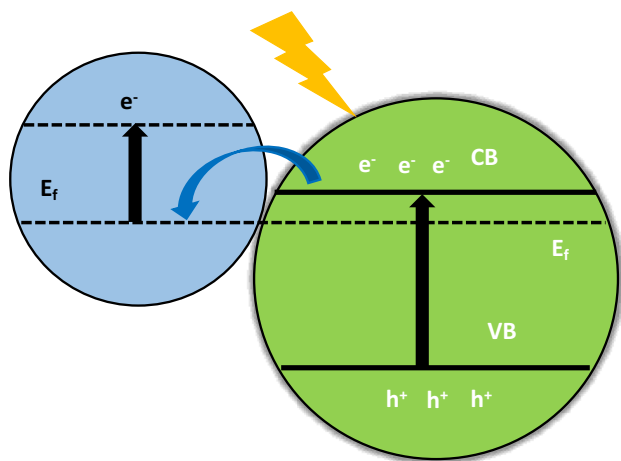


**Fig. 10** Schematic of Schottky junction (Rajbongshi 2020)

### Z-scheme photocatalytic structure

As demonstrated in Fig. 11, Z-scheme is a particular kind of heterojunction, where two materials are separated by a redox mediator with flexible oxidation conditions. Zhou et al., first suggested a Z-scheme photocatalyst for water splitting (Zhou et al. 2021).  $\text{NO}_2^-/\text{NO}_3^-$ ,  $\text{I}^-/\text{IO}_3^-$  and  $\text{Fe}^{2+}/\text{Fe}^{3+}$  are considered reversible redox mediators, which are commonly utilized in the Z-scheme. The redox mediator Z-scheme has three parts: a pair of donor/acceptor molecules, photosystem I (PSI), and photosystem II (PSII). Donor–acceptor facilitates electrons transformation from the conduction band of one photosystem to the valence band of another photosystem to recombination with a hole (Li et al. 2016).

Nevertheless, it has several disadvantages: absorbing a certain portion of the visible light and causing different unfavorable reactions, thus decreasing light absorption in the photocatalyst surface. As a result, the direct Z-scheme without redox mediator is an effective candidate since the photoexcited electrons during solar light in photosystem II might be recombined with the hole in the valence band of photosystem I. Hence, in comparison with photosystem II, the valence band of photosystem I must be relatively higher, and in comparison, with photosystem I, the conduction band of photosystem II must be relatively lower. Because of that, higher reductive electrons and oxidative holes can be produced in two various sections, causing an improvement in the photocatalytic activity (Rajbongshi et al. 2015).

### Semiconductor–semiconductor (S–S) heterojunction

S/S heterojunction is an effective method to obtain active, visible photocatalysts. Non-p-n and p-n junction are two kinds of semiconductor/semiconductor heterojunction. In p-n heterojunction, n- and p-type materials are in contact; the diffusion of holes and electrons can generate a space charge area, and the built-in potential in the interface of

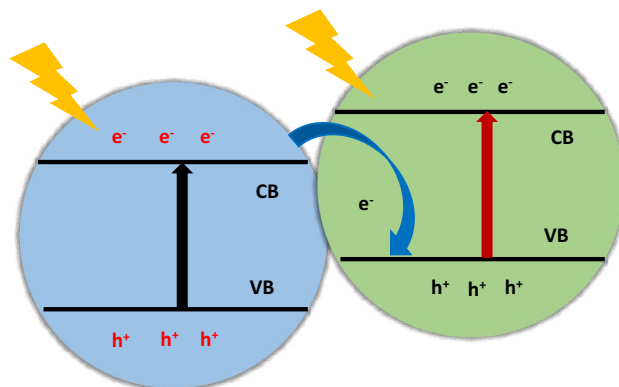


**Fig. 11** Z-scheme of a heterojunction photocatalyst (Rajbongshi 2020)

the two semiconductors which facilitates charge separation. Holes and electrons are produced when photons with energy equal to the material bandgap react with the p-n heterojunction. As demonstrated in Fig. 12, such electrons and holes are separated by the electrical field, and thus the recombination of the charges is minimum. Some of the significant benefits of the p-n heterojunction photocatalysts are higher carrier lifetime, a rapid charge transformation, and efficient electron–hole separation. Various semiconductors like graphene oxide, ZnO, and Cu<sub>2</sub>O demonstrate a remarkable enhancement in the photocatalysis activity in the p-n heterojunction with titanium oxide (Rajbongshi et al. 2015).

### Controlling of morphology

It is apparent that when the surface area is high, the particle size is smaller, and as a result, the number of active sites is more significant. However, usually smaller particle sizes cannot demonstrate significant catalytic performance. Moreover, particle morphology can influence the surface area and, as a result, the processing activity. A proper degree of concentration is essential in order to move the charges from the core particle to the surface, which is significantly related to the surface properties, design, and morphology. Many investigations have been conducted on the influence of morphology on photocatalytic activity. Tubes, belts, and wires, which are one-dimensional nanostructures because of their specific chemical, optical, and electronic properties as compared to their bulk counterparts, have demonstrated significant improvement in photocatalytic activity. One-dimensional nanostructure improves the surface area in a photocatalytic process and the carrier collection performance (Rajbongshi and Samdarshi 2014). Also, one-dimensional structures limit the progress of the electrons in one direction because of the decreasing recombination rate. Moreover, hierarchical nanostructure combination is a probable technique since interrelated pore structure, significant surface area, and great porosity improve light absorption

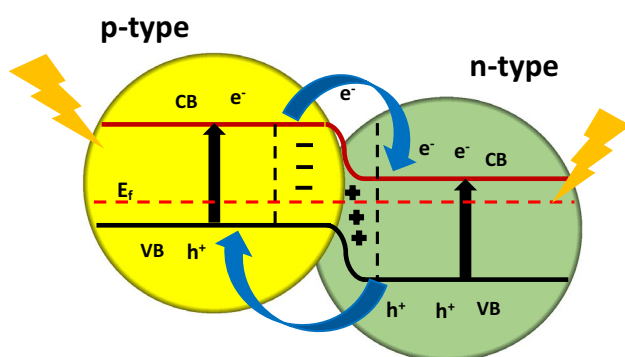


Fig. 12 p-n heterojunction junction (Rajbongshi 2020)

and optimum transportation of charge. Bio-templating is an efficient approach to achieve morphology-governable materials with functional specialties, complications, and relevant specific properties. By selecting templating with a proper morphology, the ultimate system can be regulated, which is considered as the benefit of bio-templating (Herrera-Beurnio et al. 2021).

### Conclusion and future research direction

Ever-growing different kinds of water-related pollutants are regarded as the most considerable challenge in the contemporary world. The enhancement of sophisticated technologies plays a pivotal role in alleviating water-related concerns. However, increasing anthropogenic and industrial-driven activities produce substantial volumes of different kinds of contaminants which potentially can pose significant hazards to both environment and human beings. As a result, the efficient removal of various types of pollutants in an aqueous environment is of prime concern which following that a growing demand for the advent of highly sophisticated and cost-effective wastewater treatment methods is inevitable. In this vein, as previously discussed, the photocatalyst process has the excellent ability to remove and mineralize various contaminants completely and efficiently, which renders it a competitive alternative for traditional wastewater treatment methods.

However, the presence of several major challenges which required to be properly overcome forced the research community toward further exploration. To be more specific, regardless of outstanding enhancements in the photocatalytic process, it is obvious that developing various materials with enhanced efficiency is still problematic. The future investigation is required to predominantly concentrate on entire critical areas like thermodynamic kinetics, the chemistry of interface and surface, charge separation, and transformation besides light absorption. Following are some recommendations for further explorations.

- *Industrialized photocatalysis process:* In order to make this method industrialized, the significant challenge is the stability, cost, and wide-ranging production of the photocatalyst. Aiming to the industrialization of this promising method and overcoming these serious challenges, urgent and comprehensive research efforts is required.
- *Novel materials for improving process efficiency:* Although inorganic semiconductor-dependent systems have obtained substantial enhancement, different innovative and enhanced materials must be utilized in the operation of photocatalytic process. Still, further investigation is required for modification of available materials for yielding maximum process efficiency, although several



novel materials like graphene, graphitic carbon nitrides, and integrated metallic and organic structures have been successfully used in the photocatalytic processes.

- *The temperature of the process*: During the photocatalytic systems by application of visible or ultraviolet light, there is an increase in the regional temperature which can potentially influence the kinetics and thermodynamics properties of the surface reaction and the total performance of the photocatalytic system. Hence, for improving the system efficiency, the photo-induced increased temperature of the process must be the focus of attention for process optimization.

In the cause of integration of photocatalyst with the effective adsorbents, although their synergistic effects overcomes several disadvantages of the individual photocatalytic process, still several issues required to be regarded for industrialization like reusability, temperature, and pH. Moreover, further rigorous attempts are required to discover or develop the excellent operations, for instance, fluidized bed reactor or annular photocatalytic reactor to utilize integrated photocatalysis adsorbents as suspended solids for degradation of different kinds of organic pollutants. Improving the photocatalyst activity is the primary purpose of a combination of photocatalysis with various types of adsorbents. However, the major restriction of this method is separation for improving the reusability of the suspension-dependent photocatalytic process. Since magnetic separation avoids the sedimentation and agglomeration of photocatalyst nanoparticles besides presenting a simple and easy approach for removing and recycling the magnetic particles, it has garnered significant attention. Furthermore, suspending the composite in the membrane can enable the easy agglomeration of integrated photocatalysis adsorbents after each treatment process. Therefore, further research attempts are required to develop the aforesaid methods for rendering such a promising technology absolutely reliable.

Moreover, regarding the toxic nature of different photocatalysts, the entire separation of the catalyst from the solution environment is needed more investigation. In this way, concentrating on the influence of fixed bed heterogeneous catalysts can be optimistic approach. Also, detecting appropriate photocatalyst with reduced amounts of the bandgap is in demand for the energy saving aims. In spite of the fast development in removal technologies, removing operational challenges should be a focus of attention to the full-scale and practical enhancement of installed photocatalyst reactors. For instance, emergence of high-tech reactors for detecting and observing instruments in the entire treatment operation.

All in all, considering the above-mentioned recommendations, it can be concluded that the photocatalyst method still needs many explorations for wide-ranging applications

in wastewater treatment besides acting as a reliable technology for overcoming previously discussed serious barriers.

## References

- Afeesh R, Barakat NAM, Al-Deyab SS et al (2012) Nematic shaped cadmium sulfide doped electrospun nanofiber mat: highly efficient, reusable, solar light photocatalyst. *Colloids Surf A Physicochem Eng Asp* 409:21–29. <https://doi.org/10.1016/j.colsurfa.2012.05.021>
- Aghaeinejad-Meybodi A, Ebadi A, Khataee A, Dehghani Kiadehi A (2021) Comparative investigation on catalytic ozonation of fluoxetine antidepressant drug in the presence of boehmite and  $\gamma$ -alumina nanocatalysts: operational parameters, kinetics and degradation mechanism studies. *Chem Pap* 75:421–430. <https://doi.org/10.1007/s11696-020-01312-0>
- Ahmad M, Ahmed E, Hong ZL et al (2013) Graphene-Ag/ZnO nanocomposites as high performance photocatalysts under visible light irradiation. *J Alloys Compd* 577:717–727. <https://doi.org/10.1016/j.jallcom.2013.06.137>
- Ahmad S, Aadil M, Ejaz SR et al (2022) Sol-gel synthesis of nanostructured ZnO/SrZnO<sub>2</sub> with boosted antibacterial and photocatalytic activity. *Ceram Int* 48:2394–2405. <https://doi.org/10.1016/J.CERAMINT.2021.10.020>
- Akerdi AG, Bahrami SH (2019) Application of heterogeneous nanosemiconductors for photocatalytic advanced oxidation of organic compounds: a review. *J Environ Chem Eng* 7:103283. <https://doi.org/10.1016/J.JECE.2019.103283>
- Akerdi AG, Bahrami SH, Arami M, Pajootan E (2016) Photocatalytic discoloration of Acid Red 14 aqueous solution using titania nanoparticles immobilized on graphene oxide fabricated plate. *Chemosphere* 159:293–299. <https://doi.org/10.1016/j.chemosphere.2016.06.020>
- Akkari M, Aranda P, Ben Rhaiem H et al (2016) ZnO/clay nanoarchitectures: Synthesis, characterization and evaluation as photocatalysts. *Appl Clay Sci* 131:131–139. <https://doi.org/10.1016/j.clay.2015.12.013>
- Alamelu K, Jaffar Ali BM (2018) TiO<sub>2</sub>-Pt composite photocatalyst for photodegradation and chemical reduction of recalcitrant organic pollutants. *J Environ Chem Eng* 6:5720–5731. <https://doi.org/10.1016/j.jece.2018.08.042>
- Alansi AM, Al-Qunaibit M, Alade IO et al (2018) Visible-light responsive BiOBr nanoparticles loaded on reduced graphene oxide for photocatalytic degradation of dye. *J Mol Liq* 253:297–304. <https://doi.org/10.1016/j.molliq.2018.01.034>
- Alhaddad M, Shawky A, Zaki ZI (2021) Reduced graphene oxide-supported PbTiO<sub>3</sub> nanospheres: improved ceramic photocatalyst toward enriched photooxidation of thiophene by visible light. *Mol Catal* 499:111301. <https://doi.org/10.1016/J.MCAT.2020.111301>
- Ali W, Ullah H, Zada A et al (2020) Synthesis of TiO<sub>2</sub> modified self-assembled honeycomb ZnO/SnO<sub>2</sub> nanocomposites for exceptional photocatalytic degradation of 2,4-dichlorophenol and bisphenol A. *Sci Total Environ* 746:141291. <https://doi.org/10.1016/J.SCITOTENV.2020.141291>
- Alim SA, Rao TS, Raju IM et al (2019) Fabrication of visible light driven nano structured Copper, Boron codoped TiO<sub>2</sub> for photocatalytic removal of Lissamine Green B. *J Saudi Chem Soc* 23:92–103. <https://doi.org/10.1016/j.jscs.2018.05.005>
- Al-Shalalfeh MM, Onawole AT, Saleh TA, Al-Saadi AA (2017) Spherical silver nanoparticles as substrates in surface-enhanced Raman spectroscopy for enhanced characterization of ketoconazole.

- Mater Sci Eng C 76:356–364. <https://doi.org/10.1016/j.msec.2017.03.081>
- Anirudhan TS, Shainy F, Christa J (2017) Synthesis and characterization of polyacrylic acid-grafted-carboxylic graphene/titanium nanotube composite for the effective removal of enrofloxacin from aqueous solutions: adsorption and photocatalytic degradation studies. *J Hazard Mater* 324:117–130. <https://doi.org/10.1016/j.jhazmat.2016.09.073>
- Ashour AF, El-Awady AT, Tawfik MA (2022) Numerical investigation on the thermal performance of a flat plate solar collector using ZnO & CuO water nanofluids under Egyptian weathering conditions. *Energy* 240:122743. <https://doi.org/10.1016/J.ENERGY.2021.122743>
- Bahnemann D, Bockelmann D, Goslich R (1991) Mechanistic studies of water detoxification in illuminated TiO<sub>2</sub> suspensions. *Sol Energy Mater* 24:564–583. [https://doi.org/10.1016/0165-1633\(91\)90091-X](https://doi.org/10.1016/0165-1633(91)90091-X)
- Bashir B, Khalid MU, Aadil M et al (2021) Cu<sub>x</sub>Ni<sub>1-x</sub> nanostructures and their nanocomposites with reduced graphene oxide: synthesis, characterization, and photocatalytic applications. *Ceram Int* 47:3603–3613. <https://doi.org/10.1016/J.CERAMINT.2020.09.209>
- Bera S, Pal M, Naskar A, Jana S (2016) Hierarchically structured ZnO-graphene hollow microspheres towards effective reusable adsorbent for organic pollutant via photodegradation process. *J Alloys Compd* 669:177–186. <https://doi.org/10.1016/j.jallcom.2016.02.007>
- Bettinelli M, Dallacasa V, Falcomer D et al (2007) Photocatalytic activity of TiO<sub>2</sub> doped with boron and vanadium. *J Hazard Mater* 146:529–534. <https://doi.org/10.1016/j.jhazmat.2007.04.053>
- Bhatia S, Verma N, Bedi RK (2017) Effect of aging time on gas sensing properties and photocatalytic efficiency of dye on In-Sn co-doped ZnO nanoparticles. *Mater Res Bull* 88:14–22. <https://doi.org/10.1016/j.materresbull.2016.12.011>
- Bie C, Yu H, Cheng B et al (2021) Design, fabrication, and mechanism of nitrogen-doped graphene-based photocatalyst. *Adv Mater* 33:2003521. <https://doi.org/10.1002/ADMA.202003521>
- Boningari T, Inturi SNR, Suidan M, Smirniotis PG (2018) Novel one-step synthesis of sulfur doped-TiO<sub>2</sub> by flame spray pyrolysis for visible light photocatalytic degradation of acetaldehyde. *Chem Eng J* 339:249–258. <https://doi.org/10.1016/j.cej.2018.01.063>
- Bouna L, Rhouta B, Maury F (2013) Physicochemical study of photocatalytic activity of TiO<sub>2</sub> supported palygorskite clay mineral. *Int J Photoenergy*. <https://doi.org/10.1155/2013/815473>
- Burns RA, Crittenden JC, Hand DW et al (1999) Effect of inorganic ions in heterogeneous photocatalysis of TCE. *J Environ Eng* 125:77–85. [https://doi.org/10.1061/\(asce\)0733-9372\(1999\)125:1\(77\)](https://doi.org/10.1061/(asce)0733-9372(1999)125:1(77))
- Chen Y, Liu K (2016) Preparation and characterization of nitrogen-doped TiO<sub>2</sub>/diatomite integrated photocatalytic pellet for the adsorption-degradation of tetracycline hydrochloride using visible light. *Chem Eng J* 302:682–696. <https://doi.org/10.1016/j.cej.2016.05.108>
- Chen Z, Li D, Zhang W et al (2009) Photocatalytic degradation of dyes by ZnIn<sub>2</sub>S<sub>4</sub> microspheres under visible light irradiation. *J Phys Chem C* 113:4433–4440. <https://doi.org/10.1021/jp8092513>
- Chen FP, Jin GP, Su JY, Feng X (2016) Electrochemical preparation of uniform CuO/Cu<sub>2</sub>O heterojunction on β-cyclodextrin-modified carbon fibers. *J Appl Electrochem* 46:379–388. <https://doi.org/10.1007/s10800-016-0926-4>
- Chen F, Ma T, Zhang T et al (2021) Atomic-level charge separation strategies in semiconductor-based photocatalysts. *Adv Mater* 33:2005256. <https://doi.org/10.1002/ADMA.202005256>
- Cheng H, Wang J, Zhao Y, Han X (2014) Effect of phase composition, morphology, and specific surface area on the photocatalytic activity of TiO<sub>2</sub> nanomaterials. *RSC Adv* 4:47031–47038. <https://doi.org/10.1039/c4ra05509h>
- Chkirida S, Zari N, Achour R et al (2021) Highly synergic adsorption/photocatalytic efficiency of Alginate/Bentonite impregnated TiO<sub>2</sub> beads for wastewater treatment. *J Photochem Photobiol A Chem* 412:113215. <https://doi.org/10.1016/J.JPHOTOCHEM.2021.113215>
- Choi H, Stathatos E, Dionysiou DD (2006) Sol-gel preparation of mesoporous photocatalytic TiO<sub>2</sub> films and TiO<sub>2</sub>/Al<sub>2</sub>O<sub>3</sub> composite membranes for environmental applications. *Appl Catal B Environ* 63:60–67. <https://doi.org/10.1016/j.apcatb.2005.09.012>
- Chong MN, Lei S, Jin B et al (2009) Optimisation of an annular photoreactor process for degradation of Congo Red using a newly synthesized titania impregnated kaolinite nano-photocatalyst. *Sep Purif Technol* 67:355–363. <https://doi.org/10.1016/j.seppur.2009.04.001>
- De Opereira L, De Moura SG, Coelho GCM et al (2019) Magnetic photocatalysts from industrial residues and TiO<sub>2</sub> for the degradation of organic contaminants. *J Environ Chem Eng* 7:102826. <https://doi.org/10.1016/j.jece.2018.102826>
- Erjavec B, Hudoklin P, Perc K et al (2016) Glass fiber-supported TiO<sub>2</sub> photocatalyst: Efficient mineralization and removal of toxicity/estrogenicity of bisphenol A and its analogs. *Appl Catal B Environ* 183:149–158. <https://doi.org/10.1016/j.apcatb.2015.10.033>
- Ersan G, Kaya Y, Apul OG, Karanfil T (2015) Adsorption of organic contaminants by graphene nanosheets, carbon nanotubes and granular activated carbons under natural organic matter preloading conditions. *Sci Total Environ* 565:811–817. <https://doi.org/10.1016/j.scitotenv.2016.03.224>
- Fan C, Liu Q, Ma T et al (2016) Fabrication of 3D CeVO<sub>4</sub>/graphene aerogels with efficient visible-light photocatalytic activity. *Ceram Int* 42:10487–10492. <https://doi.org/10.1016/j.ceramint.2016.03.072>
- Fernandez ME, Ledesma B, Román S et al (2015) Development and characterization of activated hydrochars from orange peels as potential adsorbents for emerging organic contaminants. *Bioreour Technol* 183:221–228. <https://doi.org/10.1016/j.biortech.2015.02.035>
- Ferreira VRA, Santos PRM, Silva CIQ, Azenha MA (2021) Latest developments on TiO<sub>2</sub>-based photocatalysis: a special focus on selectivity and hollowness for enhanced photonic efficiency. *Appl Catal A Gen* 623:118243. <https://doi.org/10.1016/J.APCATA.2021.118243>
- Fletcher AJ, Uygun Y, Mark Thomas K (2007) Role of surface functional groups in the adsorption kinetics of water vapor on microporous activated carbons. *J Phys Chem C* 111:8349–8359. <https://doi.org/10.1021/jp070815v>
- Fostier AH, Pereira M, do SS, Rath S, Guimarães JR, (2008) Arsenic removal from water employing heterogeneous photocatalysis with TiO<sub>2</sub> immobilized in PET bottles. *Chemosphere* 72:319–324. <https://doi.org/10.1016/j.chemosphere.2008.01.067>
- Fu Y, Yin Z, Qin L et al (2022) Recent progress of noble metals with tailored features in catalytic oxidation for organic pollutants degradation. *J Hazard Mater* 422:126950. <https://doi.org/10.1016/J.JHAZMAT.2021.126950>
- Gamage McEvoy J, Zhang Z (2016) Synthesis and characterization of Ag/AgBr-activated carbon composites for visible light induced photocatalytic detoxification and disinfection. *J Photochem Photobiol A Chem* 321:161–170. <https://doi.org/10.1016/j.jphotochem.2016.02.004>
- Gao J, Zhang F, Xue H et al (2021) In-situ synthesis of novel ternary CdS/PdAg/g-C<sub>3</sub>N<sub>4</sub> hybrid photocatalyst with significantly enhanced hydrogen production activity and catalytic mechanism exploration. *Appl Catal B Environ* 281:119509. <https://doi.org/10.1016/J.APCATB.2020.119509>

- Ghosh A, Mondal A (2015) Fabrication of stable, efficient and recyclable p-CuO/n-ZnO thin film heterojunction for visible light driven photocatalytic degradation of organic dyes. *Mater Lett* 164:221–224. <https://doi.org/10.1016/j.matlet.2015.10.148>
- Gnanaprakasam A, Sivakumar VM, Thirumarimurugan M (2015) Influencing parameters in the photocatalytic degradation of organic effluent via nanometal oxide catalyst: a review. *Indian J Mater Sci* 2015:1–16. <https://doi.org/10.1155/2015/601827>
- Gomez S, Marchena CL, Renzini MS et al (2015) In situ generated TiO<sub>2</sub> over zeolitic supports as reusable photocatalysts for the degradation of dichlorvos. *Appl Catal B Environ* 162:167–173. <https://doi.org/10.1016/j.apcatb.2014.06.047>
- He Z, Que W, Chen J et al (2012) Photocatalytic degradation of methyl orange over nitrogen-fluorine codoped TiO<sub>2</sub> nanobelts prepared by solvothermal synthesis. *ACS Appl Mater Interfaces* 4:6816–6826. <https://doi.org/10.1021/am3019965>
- Hegazi HA (2013) Removal of heavy metals from wastewater using agricultural and industrial wastes as adsorbents. *HBRC J* 9:276–282. <https://doi.org/10.1016/j.hbrj.2013.08.004>
- Heidari M, Bahrami H, Ranjbar-Mohammadi M (2017) Fabrication, optimization and characterization of electrospun poly(caprolactone)/gelatin/graphene nanofibrous mats. *Mater Sci Eng C* 78:218–229. <https://doi.org/10.1016/j.msec.2017.04.095>
- Hekmatshoar R, Yari AR, Shokri A (2020) Using ZnO based on Bentonite as a nano photocatalyst for degradation of Acid Red 114 in synthetic wastewater. *J Nanoanal.* <https://doi.org/10.22034/jna>
- Herath A, Navarathna C, Warren S et al (2022) Iron/titanium oxide-biochar (Fe<sub>2</sub>TiO<sub>5</sub>/BC): a versatile adsorbent/photocatalyst for aqueous Cr(VI), Pb<sup>2+</sup>, F<sup>-</sup> and methylene blue. *J Colloid Interface Sci.* <https://doi.org/10.1016/J.JCIS.2022.01.067>
- Herrera-Beurnio MC, Hidalgo-Carrillo J, López-Tenllado FJ et al (2021) Bio-templating: an emerging synthetic technique for catalysts: a review. *Catalysts* 11:1364. <https://doi.org/10.3390/CATAL11111364>
- Hu S, Ma L, You J et al (2014) Enhanced visible light photocatalytic performance of g-C<sub>3</sub>N<sub>4</sub> photocatalysts co-doped with iron and phosphorus. *Appl Surf Sci* 311:164–171. <https://doi.org/10.1016/j.apsusc.2014.05.036>
- Huang D, Miyamoto Y, Ding J et al (2011) A new method to prepare high-surface-area N-TiO<sub>2</sub>/activated carbon. *Mater Lett* 65:326–328. <https://doi.org/10.1016/j.matlet.2010.10.025>
- Huang Q, Liu M, Mao L et al (2017) Surface functionalized SiO<sub>2</sub> nanoparticles with cationic polymers via the combination of mussel inspired chemistry and surface initiated atom transfer radical polymerization: characterization and enhanced removal of organic dye. *J Colloid Interface Sci* 499:170–179. <https://doi.org/10.1016/j.jcis.2017.03.102>
- Huang L, Liu M, Huang H et al (2018a) Recent advances and progress on melanin-like materials and their biomedical applications. *Biomacromol* 19:1858–1868. <https://doi.org/10.1021/acs.biomac.8b00437>
- Huang Q, Zhao J, Liu M et al (2018b) Preparation of polyethylene polyamine@tannic acid encapsulated MgAl-layered double hydroxide for the efficient removal of copper (II) ions from aqueous solution. *J Taiwan Inst Chem Eng* 82:92–101. <https://doi.org/10.1016/j.jtice.2017.10.019>
- Huang Q, Zhao J, Liu M et al (2018c) Synthesis of polyacrylamide immobilized molybdenum disulfide (MoS<sub>2</sub>@PDA@PAM) composites via mussel-inspired chemistry and surface-initiated atom transfer radical polymerization for removal of copper (II) ions. *J Taiwan Inst Chem Eng* 86:174–184. <https://doi.org/10.1016/j.jtice.2017.12.027>
- Huang Y, Zhu Y, Chen S et al (2021) Schottky junctions with Bi cocatalyst for taming aqueous phase N<sub>2</sub> reduction toward enhanced solar ammonia production. *Adv Sci* 8:2003626. <https://doi.org/10.1002/ADVS.202003626>
- Jaime-Acuña OE, Villavicencio H, Petranovskii V, Raymond-Herrera O (2016) Disperse orange 30 dye degradation by assisted plasmonic photocatalysis using Ag-CdZnSO/zeolitic matrix nanocomposites. *Catal Commun* 75:103–107. <https://doi.org/10.1016/j.catcom.2015.11.009>
- Jallouli N, Pastrana-Martínez LM, Ribeiro AR et al (2018) Heterogeneous photocatalytic degradation of ibuprofen in ultrapure water, municipal and pharmaceutical industry wastewaters using a TiO<sub>2</sub>/UV-LED system. *Chem Eng J* 334:976–984. <https://doi.org/10.1016/j.cej.2017.10.045>
- Jing Y, Yin H, Li C et al (2022) Fabrication of Pt doped TiO<sub>2</sub>-ZnO@ZIF-8 core@shell photocatalyst with enhanced activity for phenol degradation. *Environ Res* 203:111819. <https://doi.org/10.1016/j.envres.2021.111819>
- Jo WK, Tayade RJ (2016) Facile photocatalytic reactor development using nano-TiO<sub>2</sub> immobilized mosquito net and energy efficient UVLED for industrial dyes effluent treatment. *J Environ Chem Eng* 4:319–327. <https://doi.org/10.1016/j.jece.2015.11.024>
- Jonidi Jafari A, Esrafil A, Rezaei Kalantari R, Banafsheh Afshan S (2021) Simultaneous removal of phenol and chromium reduction from the aqueous solution with photocatalytic process in the presence of ZnO-activated carbon fibre composite. *Int J Environ Anal Chem.* <https://doi.org/10.1080/03067319.2020.1867720>
- Kamal T, Ul-Islam M, Khan SB, Asiri AM (2015) Adsorption and photocatalyst assisted dye removal and bactericidal performance of ZnO/chitosan coating layer. *Int J Biol Macromol* 81:584–590. <https://doi.org/10.1016/j.ijbiomac.2015.08.060>
- Kamat PV (2011) Graphene-based nanoassemblies for energy conversion. *J Phys Chem Lett* 2:242–251. <https://doi.org/10.1021/jz101639v>
- Kanarakaju D, Kockler J, Motti CA et al (2015) Titanium dioxide/zeolite integrated photocatalytic adsorbents for the degradation of amoxicillin. *Appl Catal B Environ* 166–167:45–55. <https://doi.org/10.1016/j.apcatb.2014.11.001>
- Karan NS, Sarma DD, Kadam RM, Pradhan N (2010) Doping transition metal (Mn or Cu) ions in semiconductor nanocrystals. *J Phys Chem Lett* 1:2863–2866. <https://doi.org/10.1021/jz1012164>
- Karimi S, Shokri A (2021) The removal of Hexavalent chromium; (Cr (VI)) by ZnO/LECA as a nano photocatalyst using full factorial experimental design. *J Nanoanal* 8:167–175. <https://doi.org/10.22034/jna.001>
- Khalid NR, Ahmed E, Rasheed A et al (2015) Co-doping effect of carbon and yttrium on photocatalytic activity of TiO<sub>2</sub> nanoparticles for methyl orange degradation. *J Ovonic Res* 11:107–112
- Khaliliani H, Behpour M, Atouf V, Hosseini SN (2015) Immobilization of S, N-codoped TiO<sub>2</sub> nanoparticles on glass beads for photocatalytic degradation of methyl orange by fixed bed photoreactor under visible and sunlight irradiation. *Sol Energy* 112:239–245. <https://doi.org/10.1016/j.solener.2014.12.007>
- Khan M, Cao W (2013) Preparation of Y-doped TiO<sub>2</sub> by hydrothermal method and investigation of its visible light photocatalytic activity by the degradation of methylene blue. *J Mol Catal A Chem* 376:71–77. <https://doi.org/10.1016/j.molcata.2013.04.009>
- Khatamian M, Hashemian S, Sabae S (2010) Preparation and photocatalytic activity of nano-TiO<sub>2</sub>ZSM-5 composite. *Mater Sci Semicond Process* 13:156–161. <https://doi.org/10.1016/j.mssp.2010.10.002>
- Klauck CR, Giacobbo A, de Oliveira EDL et al (2017) Evaluation of acute toxicity, cytotoxicity and genotoxicity of landfill leachate treated by biological lagoon and advanced oxidation processes. *J Environ Chem Eng* 5:6188–6193. <https://doi.org/10.1016/j.jece.2017.11.058>
- Kumar A (2017) A review on the factors affecting the photocatalytic degradation of hazardous materials. *Mater Sci Eng Int J.* <https://doi.org/10.15406/msej.2017.01.00018>



- Kumar S, Davis AP (1997) Heterogeneous photocatalytic oxidation of nitrotoluenes. *Water Environ Res* 69:1238–1245. <https://doi.org/10.2175/106143097x125993>
- Lan H, Zhang G, Zhang H et al (2017) Solvothermal synthesis of BiOI flower-like microspheres for efficient photocatalytic degradation of BPA under visible light irradiation. *Catal Commun* 98:9–12. <https://doi.org/10.1016/j.catcom.2017.02.028>
- Lee CH, Shie JL, Yang YT, Chang CY (2016) Photoelectrochemical characteristics, photodegradation and kinetics of metal and non-metal elements co-doped photocatalyst for pollution removal. *Chem Eng J* 303:477–488. <https://doi.org/10.1016/j.cej.2016.05.140>
- Lee YY, Moon JH, Choi YS et al (2017) Visible-light driven photocatalytic degradation of organic dyes over ordered mesoporous  $Cd_xZn_{1-x}S$  materials. *J Phys Chem C* 121:5137–5144. <https://doi.org/10.1021/acs.jpcc.7b00038>
- Li H, Tu W, Zhou Y, Zou Z (2016) Z-scheme photocatalytic systems for promoting photocatalytic performance: recent progress and future challenges. *Adv Sci* 3:1500389. <https://doi.org/10.1002/adv.201500389>
- Li H, Li W, Wang F et al (2017a) Fabrication of two lanthanides co-doped  $Bi_2MoO_6$  photocatalyst: selection, design and mechanism of  $Ln_1/Ln_2$  redox couple for enhancing photocatalytic activity. *Appl Catal B Environ* 217:378–387. <https://doi.org/10.1016/j.apcatb.2017.06.015>
- Li H, Yang Z, Zhang J et al (2017b) Indium doped BiOI nanosheets: preparation, characterization and photocatalytic degradation activity. *Appl Surf Sci* 423:1188–1197. <https://doi.org/10.1016/j.apsusc.2017.06.301>
- Li M, Hu Q, Shan H et al (2021) Fabrication of copper phthalocyanine/reduced graphene oxide nanocomposites for efficient photocatalytic reduction of hexavalent chromium. *Chemosphere* 263:128250. <https://doi.org/10.1016/j.chemosphere.2020.128250>
- Lightcap IV, Kosel TH, Kamat PV (2010) Anchoring semiconductor and metal nanoparticles on a two-dimensional catalyst mat. storing and shuttling electrons with reduced graphene oxide. *Nano Lett* 10:577–583. <https://doi.org/10.1021/nl9035109>
- Lin YT, Weng CH, Lin YH et al (2013) Effect of C content and calcination temperature on the photocatalytic activity of C-doped  $TiO_2$  catalyst. *Sep Purif Technol* 116:114–123. <https://doi.org/10.1016/j.seppur.2013.05.018>
- Liu M, Ji J, Zhang X et al (2015) Self-polymerization of dopamine and polyethyleneimine: novel fluorescent organic nanopores for biological imaging applications. *J Mater Chem B* 3:3476–3482. <https://doi.org/10.1039/c4tb02067g>
- Liu M, Hou L, an, Xi B dou, et al (2016) Magnetically separable Ag/AgCl-zero valent iron particles modified zeolite X heterogeneous photocatalysts for tetracycline degradation under visible light. *Chem Eng J* 302:475–484. <https://doi.org/10.1016/j.cej.2016.05.083>
- Liu Y, Huang H, Gan D et al (2018) A facile strategy for preparation of magnetic graphene oxide composites and their potential for environmental adsorption. *Ceram Int* 44:18571–18577. <https://doi.org/10.1016/j.ceramint.2018.07.081>
- Liu S, Jiang X, Waterhouse GIN et al (2022) Efficient photoelectrocatalytic degradation of azo-dyes over polypyrrole/titanium oxide/reduced graphene oxide electrodes under visible light: performance evaluation and mechanism insights. *Chemosphere* 288:132509. <https://doi.org/10.1016/j.chemosphere.2021.132509>
- Macht F, Eusterhues K, Pronk GJ, Totsche KU (2011) Specific surface area of clay minerals: comparison between atomic force microscopy measurements and bulk-gas ( $N_2$ ) and -liquid (EGME) adsorption methods. *Appl Clay Sci* 53:20–26. <https://doi.org/10.1016/j.clay.2011.04.006>
- Maeda K (2014) Rhodium-doped barium titanate perovskite as a Stable p-type semiconductor photocatalyst for hydrogen evolution under visible light. *ACS Appl Mater Interfaces* 6:2167–2173. <https://doi.org/10.1021/am405293e>
- Malengreux CM, Pirard SL, Léonard G et al (2017) Study of the photocatalytic activity of  $Fe^{3+}$ ,  $Cr^{3+}$ ,  $La^{3+}$  and  $Eu^{3+}$  single-doped and co-doped  $TiO_2$  catalysts produced by aqueous sol-gel processing. *J Alloys Compd* 691:726–738. <https://doi.org/10.1016/j.jallcom.2016.08.211>
- Marschall R, Mukherji A, Tanksale A et al (2011) Preparation of new sulfur-doped and sulfur/nitrogen co-doped  $CsTaWO_6$  photocatalysts for hydrogen production from water under visible light. *J Mater Chem* 21:8871–8879. <https://doi.org/10.1039/c0jm02549f>
- Matsuzawa S, Maneerat C, Hayata Y et al (2008) Immobilization of  $TiO_2$  nanoparticles on polymeric substrates by using electrostatic interaction in the aqueous phase. *Appl Catal B Environ* 83:39–45. <https://doi.org/10.1016/j.apcatb.2008.01.036>
- Miao F, Wang Q, Zhang LC, Shen B (2021) Magnetically separable Z-scheme  $FeSiB$  metallic glass/g- $C_3N_4$  heterojunction photocatalyst with high degradation efficiency at universal pH conditions. *Appl Surf Sci* 540:148401. <https://doi.org/10.1016/j.apsusc.2020.148401>
- Mokhtar Mohamed M, Osman G, Khairou KS (2015) Fabrication of Ag nanoparticles modified  $TiO_2$ -CNT heterostructures for enhanced visible light photocatalytic degradation of organic pollutants and bacteria. *J Environ Chem Eng* 3:1847–1859. <https://doi.org/10.1016/j.jece.2015.06.018>
- Mutalib MA, Aziz F, Jamaludin NA et al (2018) (2017) Enhancement in photocatalytic degradation of methylene blue by  $LaFeO_3$ -GO integrated photocatalyst-adsorbents under visible light irradiation. *Korean J Chem Eng* 35(35):548–556. <https://doi.org/10.1007/S11814-017-0281-0>
- Navakoteswara Rao V, Ravi P, Sathish M et al (2021) Monodispersed core/shell nanospheres of  $ZnS/NiO$  with enhanced  $H_2$  generation and quantum efficiency at versatile photocatalytic conditions. *J Hazard Mater* 413:125359. <https://doi.org/10.1016/j.jhazmat.2021.125359>
- Nguyen CH, Fu CC, Juang RS (2018) Degradation of methylene blue and methyl orange by palladium-doped  $TiO_2$  photocatalysis for water reuse: Efficiency and degradation pathways. *J Clean Prod* 202:413–427. <https://doi.org/10.1016/j.jclepro.2018.08.110>
- Nguyen-Phan TD, Shin EW, Pham VH et al (2012) Mesoporous titanate/silicate/reduced graphene oxide composites: layered structure, high surface-to-volume ratio, doping effect and application in dye removal from water. *J Mater Chem* 22:20504–20511. <https://doi.org/10.1039/c2jm33309k>
- Ohno T, Akiyoshi M, Umebayashi T et al (2004) Preparation of S-doped  $TiO_2$  photocatalysts and their photocatalytic activities under visible light. *Appl Catal A Gen* 265:115–121. <https://doi.org/10.1016/j.apcata.2004.01.007>
- Pang YL, Teh WS, Lim S et al (2020) Enhancement of adsorption-photocatalysis of malachite green using oil palm biomass-derived activated carbon/ titanium dioxide composite. *Curr Anal Chem* 17:603–617. <https://doi.org/10.2174/1573411016666200106105903>
- Pang X, Skillen N, Gunaratne N et al (2021) Removal of phthalates from aqueous solution by semiconductor photocatalysis: a review. *J Hazard Mater* 402:123461. <https://doi.org/10.1016/j.jhazmat.2020.123461>
- Peng K, Fu L, Yang H, Ouyang J (2016) Perovskite  $LaFeO_3$ /montmorillonite nanocomposites: synthesis, interface characteristics and enhanced photocatalytic activity. *Sci Rep* 6:1–10. <https://doi.org/10.1038/srep19723>
- Plodinec M, Gajović A, Jakša G et al (2014) High-temperature hydrogenation of pure and silver-decorated titanate nanotubes to increase their solar absorbance for photocatalytic

- applications. *J Alloys Compd* 591:147–155. <https://doi.org/10.1016/j.jallcom.2013.12.179>
- Pourfalahoon S, Mazaheri H, Hassani Joshaghani A, Shokri A (2021) Employing a new catalytic ozonation(O<sub>3</sub>/MnO<sub>2</sub>/CP) for degradation of nitro toluene in aqueous environment using Box-Behnken experimental design. *Iran J Chem Chem Eng* 40:804–814. <https://doi.org/10.30492/IJCCE.2020.38105>
- Pucher P, Azouani R, Kanaev A, Krammer G (2008) A photocatalytic active adsorbent for gas cleaning in a fixed bed reactor. *Int J Photoenergy*. <https://doi.org/10.1155/2008/759736>
- Qin C, Li Z, Chen G et al (2015) Fabrication and visible-light photocatalytic behavior of perovskite praseodymium ferrite porous nanotubes. *J Power Sources* 285:178–184. <https://doi.org/10.1016/j.jpowsour.2015.03.096>
- Qin Y, Zhang H, Tong Z et al (2017) A facile synthesis of Fe<sub>3</sub>O<sub>4</sub>@SiO<sub>2</sub>@ZnO with superior photocatalytic performance of 4-nitrophenol. *J Environ Chem Eng* 5:2207–2213. <https://doi.org/10.1016/j.jece.2017.04.036>
- Qing L, Rui-Zhi W (2012) Preparation and photocatalytic property of lanthanum-doped TiO<sub>2</sub> nanoparticles. *Adv Mater Res* 549:584–588. <https://doi.org/10.4028/www.scientific.net/AMR.549.584>
- Qiu W, Yang D, Xu J et al (2016) Efficient removal of Cr(VI) by magnetically separable CoFe<sub>2</sub>O<sub>4</sub>/activated carbon composite. *J Alloys Compd* 678:179–184. <https://doi.org/10.1016/j.jallcom.2016.03.304>
- Qu D, Zheng M, Du P et al (2013) Highly luminescent S, N co-doped graphene quantum dots with broad visible absorption bands for visible light photocatalysts. *Nanoscale* 5:12272–12277. <https://doi.org/10.1039/c3nr04402e>
- Radhika NP, Selvin R, Kakkar R, Umar A (2019) Recent advances in nano-photocatalysts for organic synthesis. *Arab J Chem* 12:4550–4578. <https://doi.org/10.1016/j.arabjc.2016.07.007>
- Rahman A, Urabe T, Kishimoto N (2013) Color removal of reactive procion dyes by clay adsorbents. *Procedia Environ Sci* 17:270–278. <https://doi.org/10.1016/j.proenv.2013.02.038>
- Rahmani AR, Samarghandi MR, Nematollahi D, Zamani F (2019) A comprehensive study of electrochemical disinfection of water using direct and indirect oxidation processes. *J Environ Chem Eng* 7:102785. <https://doi.org/10.1016/j.jece.2018.11.030>
- Rajbongshi BM (2020) Photocatalyst: mechanism, challenges, and strategy for organic contaminant degradation. *Handb Smart Photocatal Mater*. <https://doi.org/10.1016/b978-0-12-819049-4.00011-8>
- Rajbongshi BM, Samdarshi SK (2014) ZnO and Co-ZnO nanorods - complementary role of oxygen vacancy in photocatalytic activity of under UV and visible radiation flux. *Mater Sci Eng B Solid-State Mater Adv Technol* 182:21–28. <https://doi.org/10.1016/j.mseb.2013.11.013>
- Rajbongshi BM, Samdarshi SK, Boro B (2015) Multiphase bi-component TiO<sub>2</sub>-ZnO nanocomposite: synthesis, characterization and investigation of photocatalytic activity under different wavelengths of light irradiation. *J Mater Sci Mater Electron* 26:377–384. <https://doi.org/10.1007/s10854-014-2410-4>
- Ramandi S, Entezari MH, Ghows N (2017) Sono-synthesis of solar light responsive S-N-C-tri doped TiO<sub>2</sub> photo-catalyst under optimized conditions for degradation and mineralization of Diclofenac. *Ultrason Sonochem* 38:234–245. <https://doi.org/10.1016/j.ultsonch.2017.03.008>
- Ramezanalizadeh H, Manteghi F (2017) Immobilization of mixed cobalt/nickel metal-organic framework on a magnetic BiFeO<sub>3</sub>: a highly efficient separable photocatalyst for degradation of water pollutions. *J Photochem Photobiol A Chem* 346:89–104. <https://doi.org/10.1016/j.jphotochem.2017.05.041>
- Ravichandran K, Chidhambaram N, Gobalakrishnan S (2016) Copper and Graphene activated ZnO nanopowders for enhanced photocatalytic and antibacterial activities. *J Phys Chem Solids* 93:82–90. <https://doi.org/10.1016/j.jpcs.2016.02.013>
- Reddy PAK, Reddy PVL, Kwon E et al (2016) Recent advances in photocatalytic treatment of pollutants in aqueous media. *Environ Int* 91:94–103. <https://doi.org/10.1016/j.envint.2016.02.012>
- Reynoso-Soto EA, Pérez-Sicairo S, Reyes-Cruzaley AP et al (2013) Photocatalytic degradation of nitrobenzene using nanocrystalline TiO<sub>2</sub> photocatalyst doped with Zn ions. *J Mex Chem Soc* 57:298–305. <https://doi.org/10.29356/jmcs.v57i4.193>
- Rogé V, Guignard C, Lamblin G et al (2018) Photocatalytic degradation behavior of multiple xenobiotics using MOCVD synthesized ZnO nanowires. *Catal Today* 306:215–222. <https://doi.org/10.1016/j.cattod.2017.05.088>
- Rossner A, Snyder SA, Knappe DRU (2009) Removal of emerging contaminants of concern by alternative adsorbents. *Water Res* 43:3787–3796. <https://doi.org/10.1016/j.watres.2009.06.009>
- Rostami M, Mazaheri H, Hassani Joshaghani A, Shokri A (2019) Using experimental design to optimize the photo-degradation of P-nitro toluene by nano-TiO<sub>2</sub> in synthetic wastewater. *Int J Eng Trans B Appl* 32:1074–1081. <https://doi.org/10.5829/ije.2019.32.08b.03>
- Saghi M, Shokri A, Arastehnodeh A et al (2018) The photo degradation of methyl red in aqueous solutions by α-Fe<sub>2</sub>O<sub>3</sub>/SiO<sub>2</sub> nano photocatalyst. *J Nanoanal* 5:163–170. <https://doi.org/10.22034/JNA.2018.543608>
- Saini J, Garg VK, Gupta RK, Kataria N (2017) Removal of Orange G and Rhodamine B dyes from aqueous system using hydrothermally synthesized zinc oxide loaded activated carbon (ZnO-AC). *J Environ Chem Eng* 5:884–892. <https://doi.org/10.1016/j.jece.2017.01.012>
- Sakthivel S, Shankar MV, Palanichamy M et al (2002) Photocatalytic decomposition of leather dye: comparative study of TiO<sub>2</sub> supported on alumina and glass beads. *J Photochem Photobiol A Chem* 148:153–159. [https://doi.org/10.1016/S1010-6030\(02\)00085-0](https://doi.org/10.1016/S1010-6030(02)00085-0)
- Saleh TA (2016) Nanocomposite of carbon nanotubes/silica nanoparticles and their use for adsorption of Pb(II): from surface properties to sorption mechanism. *Desalin Water Treat* 57:10730–10744. <https://doi.org/10.1080/19443994.2015.1036784>
- Saleh TA (2018) Simultaneous adsorptive desulfurization of diesel fuel over bimetallic nanoparticles loaded on activated carbon. *J Clean Prod* 172:2123–2132. <https://doi.org/10.1016/j.jclepro.2017.11.208>
- Saleh TA, Tuzen M, Sari A (2017) Magnetic activated carbon loaded with tungsten oxide nanoparticles for aluminum removal from waters. *J Environ Chem Eng* 5:2853–2860. <https://doi.org/10.1016/j.jece.2017.05.038>
- Sarkar S, Chakraborty S, Bhattacharjee C (2015) Photocatalytic degradation of pharmaceutical wastes by alginate supported TiO<sub>2</sub> nanoparticles in packed bed photo reactor (PBPR). *Ecotoxicol Environ Saf* 121:263–270. <https://doi.org/10.1016/j.ecoenv.2015.02.035>
- Schneider J, Matsuoka M, Takeuchi M et al (2014) Understanding TiO<sub>2</sub> photocatalysis: mechanisms and materials. *Chem Rev* 114:9919–9986. <https://doi.org/10.1021/cr5001892>
- Schollée JE, Hollender J, Mc Ardell CS (2021) Characterization of advanced wastewater treatment with ozone and activated carbon using LC-HRMS based non-target screening with automated trend assignment. *Water Res* 200:117209. <https://doi.org/10.1016/J.WATRES.2021.117209>
- Seo HK, Shin HS (2015) Study on photocatalytic activity of ZnO nanodisks for the degradation of Rhodamine B dye. *Mater Lett* 159:265–268. <https://doi.org/10.1016/j.matlet.2015.06.094>
- Sephehri A, Sarrafzadeh MH (2018) Effect of nitrifiers community on fouling mitigation and nitrification efficiency in a membrane bio-reactor. *Chem Eng Process Process Intensif* 128:10–18. <https://doi.org/10.1016/j.cep.2018.04.006>



- Sha Y, Mathew I, Cui Q et al (2016) Rapid degradation of azo dye methyl orange using hollow cobalt nanoparticles. *Chemosphere* 144:1530–1535. <https://doi.org/10.1016/j.chemosphere.2015.10.040>
- Shah BR, Patel UD (2022) Reductive transformation of aqueous pollutants using heterogeneous photocatalysis: a review. *J Inst Eng Ser A* 2021:1–14. <https://doi.org/10.1007/S40030-021-00586-1>
- Shaheer ARM, Vinesh V, Lakhera SK, Neppolian B (2021) Reduced graphene oxide as a solid-state mediator in TiO<sub>2</sub>/In<sub>0.5</sub>WO<sub>3</sub> S-scheme photocatalyst for hydrogen production. *Sol Energy* 213:260–270. <https://doi.org/10.1016/J.SOLENER.2020.11.030>
- Shang M, Wang W, Sun S et al (2009) Efficient visible light-induced photocatalytic degradation of contaminant by spindle-like PANI/BiVO<sub>4</sub>. *J Phys Chem C* 113:20228–20233. <https://doi.org/10.1021/JP9067729>
- Sharma G, Dionysiou DD, Sharma S et al (2019) Highly efficient Sr/Ce/activated carbon bimetallic nanocomposite for photoinduced degradation of rhodamine B. *Catal Today* 335:437–451. <https://doi.org/10.1016/J.CATTOD.2019.03.063>
- Shokri A (2019) Employing sono-fenton process for degradation of 2-nitrophenol in aqueous environment using Box-Behnken design method and kinetic study. *Russ J Phys Chem A* 93:243–249. <https://doi.org/10.1134/S003602441902002X>
- Shokri A (2020) Using Mn based on lightweight expanded clay aggregate (LECA) as an original catalyst for the removal of NO<sub>2</sub> pollutant in aqueous environment. *Surf Interfaces* 21:100705. <https://doi.org/10.1016/J.SURFIN.2020.100705>
- Shokri A (2021) Using NiFe<sub>2</sub>O<sub>4</sub> as a nano photocatalyst for degradation of polyvinyl alcohol in synthetic wastewater. *Environ Chall* 5:100332. <https://doi.org/10.1016/j.envc.2021.100332>
- Shokri A, Fard MS (2022) A critical review in electrocoagulation technology applied for oil removal in industrial wastewater. *Chemosphere* 288:132355. <https://doi.org/10.1016/J.CHEMOSPHERE.2021.132355>
- Shokri A, Mahanpoor K (2016) Removal of ortho-toluidine from industrial wastewater by UV/TiO<sub>2</sub> process. *J Chem Health Risks* 6:213–223
- Shokri A, Mahanpoor K (2018) Using UV/ZnO process for degradation of Acid red 283 in synthetic wastewater. *Bulg Chem Commun* 50:27–32
- Shokri A, Mahanpoor K, Soodbar D (2016) Evaluation of a modified TiO<sub>2</sub> (GO-B-TiO<sub>2</sub>) photo catalyst for degradation of 4-nitrophenol in petrochemical wastewater by response surface methodology based on the central composite design. *J Environ Chem Eng* 4:585–598. <https://doi.org/10.1016/j.jece.2015.11.007>
- Shokri A, Salimi M, Abmatin T (2017) Employing photo Fenton and UV/ZnO processes for removing Reactive red 195 from aqueous environment. *Fresenius Environ Bull* 26:1560–1565
- Singh M, Kaushal S, Singh P, Sharma J (2018) Boron doped graphene oxide with enhanced photocatalytic activity for organic pollutants. *J Photochem Photobiol A Chem* 364:130–139. <https://doi.org/10.1016/j.jphotochem.2018.06.002>
- Smith YR, Kar A, Subramanian V (2009) Investigation of physicochemical parameters that influence photocatalytic degradation of methyl orange over TiO<sub>2</sub>nanotubes. *Ind Eng Chem Res* 48:10268–10276. <https://doi.org/10.1021/ie801851p>
- Sohrabnezhad S, Pourahmad A, Razavi M (2016) Silver bromide in montmorillonite as visible light-driven photocatalyst and the role of montmorillonite. *Appl Phys A Mater Sci Process* 122:1–9. <https://doi.org/10.1007/s00339-016-0349-4>
- Srinivasan A, Viraraghavan T (2010) Decolorization of dye wastewaters by biosorbents: a review. *J Environ Manag* 91:1915–1929. <https://doi.org/10.1016/j.jenvman.2010.05.003>
- Stambolova I, Shipochka M, Blaskov V et al (2012) Sprayed nanostructured TiO<sub>2</sub> films for efficient photocatalytic degradation of textile azo dye. *J Photochem Photobiol B Biol* 117:19–26. <https://doi.org/10.1016/j.jphotobiol.2012.08.006>
- Subash B, Krishnakumar B, Velmurugan R et al (2012) Synthesis of Ce co-doped Ag-ZnO photocatalyst with excellent performance for NBB dye degradation under natural sunlight illumination. *Catal Sci Technol* 2:2319–2326. <https://doi.org/10.1039/c2cy20254a>
- Sun J, Qiao L, Sun S, Wang G (2008) Photocatalytic degradation of Orange G on nitrogen-doped TiO<sub>2</sub> catalysts under visible light and sunlight irradiation. *J Hazard Mater* 155:312–319. <https://doi.org/10.1016/j.jhazmat.2007.11.062>
- Tafreshi N, Sharifnia S, Moradi Dehaghi S (2017) Box-Behnken experimental design for optimization of ammonia photocatalytic degradation by ZnO/Oak charcoal composite. *Process Saf Environ Prot* 106:203–210. <https://doi.org/10.1016/j.psep.2017.01.015>
- Takeuchi M, Deguchi J, Hidaka M et al (2009) Enhancement of the photocatalytic reactivity of TiO<sub>2</sub> nano-particles by a simple mechanical blending with hydrophobic mordenite (MOR) zeolite. *Appl Catal B Environ* 89:406–410. <https://doi.org/10.1016/j.apcatb.2008.12.022>
- Taufik A, Saleh R (2017) Synergistic effect between ternary iron–zinc–copper mixed oxides and graphene for photocatalytic water decontamination. *Ceram Int* 43:3510–3520. <https://doi.org/10.1016/j.ceramint.2016.10.176>
- Tekin G, Ersöz G, Atalay S (2018) Degradation of benzoic acid by advanced oxidation processes in the presence of Fe or Fe-TiO<sub>2</sub> loaded activated carbon derived from walnut shells: a comparative study. *J Environ Chem Eng* 6:1745–1759. <https://doi.org/10.1016/j.jece.2018.01.067>
- Tian D, Zhou H, Zhang H et al (2022) Heterogeneous photocatalyst-driven persulfate activation process under visible light irradiation: from basic catalyst design principles to novel enhancement strategies. *Chem Eng J* 428:131166. <https://doi.org/10.1016/J.CEJ.2021.131166>
- Tka N, Jabli M, Saleh TA, Salman GA (2018) Amines modified fibers obtained from natural Populus tremula and their rapid biosorption of Acid Blue 25. *J Mol Liq* 250:423–432. <https://doi.org/10.1016/j.molliq.2017.12.026>
- Tong H, Tao X, Wu D et al (2014) Preparation and characterization of doped TiO<sub>2</sub> nanofibers by coaxial electrospinning combined with sol-gel process. *J Alloys Compd* 586:274–278. <https://doi.org/10.1016/j.jallcom.2013.09.177>
- Torkian N, Bahrami A, Hosseini-Abari A et al (2021) Synthesis and characterization of Ag-ion-exchanged zeolite/TiO<sub>2</sub> nanocomposites for antibacterial applications and photocatalytic degradation of antibiotics. *Environ Res*. <https://doi.org/10.1016/J.ENVRES.2021.112157>
- Truppi A, Petronella F, Placido T et al (2019) Gram-scale synthesis of UV–vis light active plasmonic photocatalytic nanocomposite based on TiO<sub>2</sub>/Au nanorods for degradation of pollutants in water. *Appl Catal B Environ* 243:604–613. <https://doi.org/10.1016/j.apcatb.2018.11.002>
- Tryba B (2008) Increase of the photocatalytic activity of TiO<sub>2</sub> by carbon and iron modifications. *Int J Photoenergy*. <https://doi.org/10.1155/2008/721824>
- Vadivel S, Vanitha M, Muthukrishnaraj A, Balasubramanian N (2014) Graphene oxide-BiOBr composite material as highly efficient photocatalyst for degradation of methylene blue and rhodamine-B dyes. *J Water Process Eng* 1:17–26. <https://doi.org/10.1016/j.jwpe.2014.02.003>
- Vaidya S, Patra A, Ganguli AK (2010) CdS@TiO<sub>2</sub> and ZnS@TiO<sub>2</sub> core-shell nanocomposites: synthesis and optical properties. *Colloids Surf A Physicochem Eng Asp* 363:130–134. <https://doi.org/10.1016/j.colsurfa.2010.04.030>
- Van KN, Huu HT, Nguyen Thi VN et al (2022) Facile construction of S-scheme SnO<sub>2</sub>/g-C<sub>3</sub>N<sub>4</sub> photocatalyst for improved

- photoactivity. *Chemosphere* 289:133120. <https://doi.org/10.1016/J.CHEMOSPHERE.2021.133120>
- Vasseghian Y, Dragoi EN, Almomani F, Le VT (2022) Graphene-based materials for metronidazole degradation: a comprehensive review. *Chemosphere* 286:131727. <https://doi.org/10.1016/J.CHEMOSPHERE.2021.131727>
- Vimonses V, Jin B, Chow CWK, Saint C (2010) An adsorption-photocatalysis hybrid process using multi-functional-nanoporous materials for wastewater reclamation. *Water Res* 44:5385–5397. <https://doi.org/10.1016/j.watres.2010.06.033>
- Wang S, Zhou S (2011) Photodegradation of methyl orange by photocatalyst of CNTs/P-TiO<sub>2</sub> under UV and visible-light irradiation. *J Hazard Mater* 185:77–85. <https://doi.org/10.1016/j.jhazmat.2010.08.125>
- Wang J, Yin S, Komatsu M, Sato T (2005) Lanthanum and nitrogen co-doped SrTiO<sub>3</sub> powders as visible light sensitive photocatalyst. *J Eur Ceram Soc* 25:3207–3212. <https://doi.org/10.1016/j.jeurceramsoc.2004.07.027>
- Wang P, Zhai Y, Wang D, Dong S (2011) Synthesis of reduced graphene oxide-anatase TiO<sub>2</sub> nanocomposite and its improved photo-induced charge transfer properties. *Nanoscale* 3:1640–1645. <https://doi.org/10.1039/c0nr00714e>
- Wang M, Che Y, Niu C et al (2013) Effective visible light-active boron and europium co-doped BiVO<sub>4</sub> synthesized by sol-gel method for photodegradation of methyl orange. *J Hazard Mater* 262:447–455. <https://doi.org/10.1016/j.jhazmat.2013.08.063>
- Wu N (2018) Plasmonic metal-semiconductor photocatalysts and photoelectrochemical cells: a review. *Nanoscale* 10:2679–2696. <https://doi.org/10.1039/c7nr08487k>
- Wu L, Lin X, Zhou X, Luo X (2016) Removal of uranium and fluorine from wastewater by double-functional microsphere adsorbent of SA/CMC loaded with calcium and aluminum. *Appl Surf Sci* 384:466–479. <https://doi.org/10.1016/j.apsusc.2016.05.056>
- Wu Y, Gong Y, Liu J et al (2017) B and Y co-doped TiO<sub>2</sub> photocatalyst with enhanced photodegradation efficiency. *J Alloys Compd* 695:1462–1469. <https://doi.org/10.1016/j.jallcom.2016.10.284>
- Wu J, Yi S, Wang Y et al (2021) Polymer-based TiO<sub>2</sub> nanocomposite membrane: synthesis and organic pollutant removal. *Int J Smart Nano Mater* 12:129–145. <https://doi.org/10.1080/19475411.2021.1901792>
- Xiao S, Guan Y, Shang H et al (2022) An S-scheme NH<sub>2</sub>-UiO-66/SiC photocatalyst via microwave synthesis with improved CO<sub>2</sub> reduction activity. *J CO<sub>2</sub> Util* 55:101806. <https://doi.org/10.1016/J.JCOU.2021.101806>
- Xie T, Liu C, Xu L et al (2013) Novel heterojunction Bi<sub>2</sub>O<sub>3</sub>/SrFe<sub>2</sub>O<sub>9</sub> magnetic photocatalyst with highly enhanced photocatalytic activity. *J Phys Chem C* 117:24601–24610. <https://doi.org/10.1021/jp408627e>
- Xu H, Zhang D, Xu A et al (2015) Quantum sized zinc oxide immobilized on bentonite clay and degradation of C.I. Acid red 35 in aqueous under ultraviolet Light. *Int J Photoenergy*. <https://doi.org/10.1155/2015/750869>
- Xu L, Zhou Y, Wu Z et al (2017) Improved photocatalytic activity of nanocrystalline ZnO by coupling with CuO. *J Phys Chem Solids* 106:29–36. <https://doi.org/10.1016/J.JPCS.2017.03.001>
- Yadav HM, Kolekar TV, Barge AS et al (2016) Enhanced visible light photocatalytic activity of Cr<sup>3+</sup>-doped anatase TiO<sub>2</sub> nanoparticles synthesized by sol-gel method. *J Mater Sci Mater Electron* 27:526–534. <https://doi.org/10.1007/s10854-015-3785-6>
- Yahya N, Aizat A, Sahrudin MAH et al (2018a) Adsorption and photocatalytic study of integrated photocatalyst adsorbent (IPCA) using LaFeO<sub>3</sub>-GO nanocomposites for removal of synthetic dyes. *Chem Eng Trans* 63:517–522. <https://doi.org/10.3303/CET1863087>
- Yahya N, Aziz F, Jamaludin NA et al (2018b) A review of integrated photocatalyst adsorbents for wastewater treatment. *J Environ Chem Eng* 6:7411–7425. <https://doi.org/10.1016/J.JECE.2018.06.051>
- Yoon TH, Hong LY, Kim DP (2011) Photocatalytic reaction using novel inorganic polymer derived packed bed microreactor with modified TiO<sub>2</sub> microbeads. *Chem Eng J* 167:666–670. <https://doi.org/10.1016/j.cej.2010.08.090>
- Yousef A, Barakat NAM, Al-Deyab SS et al (2012) Encapsulation of CdO/ZnO NPs in PU electrospun nanofibers as novel strategy for effective immobilization of the photocatalysts. *Colloids Surf A Physicochem Eng Asp* 401:8–16. <https://doi.org/10.1016/j.colsurfa.2012.02.033>
- Yu N, Chen Y, Zhang W et al (2016a) Preparation of Yb<sup>3+</sup>/Er<sup>3+</sup> co-doped BiOCl sheets as efficient visible-light-driven photocatalysts. *Mater Lett* 179:154–157. <https://doi.org/10.1016/j.matlet.2016.05.071>
- Yu YQ, Zhang HY, Chai YQ et al (2016b) A sensitive electrochemiluminescent aptasensor based on perylene derivatives as a novel co-reaction accelerator for signal amplification. *Biosens Bioelectron* 85:8–15. <https://doi.org/10.1016/j.bios.2016.04.088>
- Zafar Z, Fatima R, Kim JO (2021) Experimental studies on water matrix and influence of textile effluents on photocatalytic degradation of organic wastewater using Fe–TiO<sub>2</sub> nanotubes: towards commercial application. *Environ Res* 197:111120. <https://doi.org/10.1016/J.ENVRES.2021.111120>
- Zargazi M, Entezari MH (2019) Anodic electrophoretic deposition of Bi<sub>2</sub>WO<sub>6</sub> thin film: high photocatalytic activity for degradation of a binary mixture. *Appl Catal B Environ* 242:507–517. <https://doi.org/10.1016/j.apcatb.2018.09.093>
- Zeng G, Huang L, Huang Q et al (2018) Rapid synthesis of MoS<sub>2</sub>-PDA-Ag nanocomposites as heterogeneous catalysts and antimicrobial agents via microwave irradiation. *Appl Surf Sci* 459:588–595. <https://doi.org/10.1016/j.apsusc.2018.07.144>
- Zhan S, Chen D, Jiao X, Tao C (2006) Long TiO<sub>2</sub> hollow fibers with mesoporous walls: Sol-gel combined electrospun fabrication and photocatalytic properties. *J Phys Chem B* 110:11199–11204. <https://doi.org/10.1021/jp057372k>
- Zhang Y, Chu W (2022) Cooperation of multi-walled carbon nanotubes and cobalt doped TiO<sub>2</sub> to activate peroxymonosulfate for antipyrine photocatalytic degradation. *Sep Purif Technol* 282:119996. <https://doi.org/10.1016/J.SEPPUR.2021.119996>
- Zhang X, Liu Q (2008) Visible-light-induced degradation of formaldehyde over titania photocatalyst co-doped with nitrogen and nickel. *Appl Surf Sci* 254:4780–4785. <https://doi.org/10.1016/j.apsusc.2008.01.094>
- Zhang S, Li J, Zeng M et al (2013) In situ synthesis of water-soluble magnetic graphitic carbon nitride photocatalyst and its synergistic catalytic performance. *ACS Appl Mater Interfaces* 5:12735–12743. <https://doi.org/10.1021/am404123z>
- Zhang M, Luo W, Wei Z et al (2016a) Separation free C<sub>3</sub>N<sub>4</sub>/SiO<sub>2</sub> hybrid hydrogels as high active photocatalysts for TOC removal. *Appl Catal B Environ* 194:105–110. <https://doi.org/10.1016/j.apcatb.2016.04.049>
- Zhang Q, Lu Z, Jin S et al (2016b) TiO<sub>2</sub> nanotube-carbon macroscopic monoliths with multimodal porosity as efficient recyclable photocatalytic adsorbents for water purification. *Mater Chem Phys* 173:452–459. <https://doi.org/10.1016/j.matchemphys.2016.02.037>
- Zhao W, Ma W, Chen C et al (2004) Efficient degradation of toxic organic pollutants with Ni<sub>2</sub>O<sub>3</sub>/TiO<sub>2</sub>-xB<sub>x</sub> under visible irradiation. *J Am Chem Soc* 126:4782–4783. <https://doi.org/10.1021/ja0396753>
- Zhao C, Zhou Y, de Ridder DJ et al (2014) Advantages of TiO<sub>2</sub>/5A composite catalyst for photocatalytic degradation of antibiotic oxytetracycline in aqueous solution: comparison between TiO<sub>2</sub> and TiO<sub>2</sub>/5A composite system. *Chem Eng J* 248:280–289. <https://doi.org/10.1016/j.cej.2014.03.050>

- Zheng GH, Zhang JW, Wang W et al (2021) Synergy effect of Lorentz force and dissolved oxygen on photocatalytic performance under magnetic field. *Dig J Nanomater Biostruct* 16:409–424
- Zhou S, Ray AK (2003) Kinetic studies for photocatalytic degradation of eosin b on a thin film of titanium dioxide. *Ind Eng Chem Res* 42:6020–6033. <https://doi.org/10.1021/ie030366v>
- Zhou W, Liu Q, Zhu Z, Zhang J (2010) Preparation and properties of vanadium-doped TiO<sub>2</sub> photocatalysts. *J Phys D Appl Phys* 43:035301. <https://doi.org/10.1088/0022-3727/43/3/035301>
- Zhou Z, Peng X, Zhong L et al (2016) Electrospun cellulose acetate supported Ag@AgCl composites with facet-dependent photocatalytic properties on degradation of organic dyes under visible-light irradiation. *Carbohydr Polym* 136:322–328. <https://doi.org/10.1016/j.carbpol.2015.09.009>
- Zhou J, Li D, Zhao W et al (2021) First-principles evaluation of volatile organic compounds degradation in Z-scheme photocatalytic systems: MXene and Graphitic-CN heterostructures. *ACS Appl Mater Interfaces* 13:23843–23852. [https://doi.org/10.1021/ACSAMI.1C05617/SUPPL\\_FILE/AM1C05617\\_SI\\_001.PDF](https://doi.org/10.1021/ACSAMI.1C05617/SUPPL_FILE/AM1C05617_SI_001.PDF)
- Zhu J, Deng Z, Chen F et al (2006) Hydrothermal doping method for preparation of Cr<sup>3+</sup>-TiO<sub>2</sub> photocatalysts with concentration gradient distribution of Cr<sup>3+</sup>. *Appl Catal B Environ* 62:329–335. <https://doi.org/10.1016/j.apcatb.2005.08.013>
- Zhu Q, Moggridge GD, Ainte M et al (2016) Adsorption of pyridine from aqueous solutions by polymeric adsorbents MN 200 and MN 500. Part 1: Adsorption performance and PFG-NMR studies. *Chem Eng J* 306:67–76. <https://doi.org/10.1016/j.cej.2016.07.039>
- Zoschke K, Börnick H, Worch E (2014) Vacuum-UV radiation at 185 nm in water treatment: a review. *Water Res* 52:131–145. <https://doi.org/10.1016/j.watres.2013.12.034>
- Zou Z, Ye J, Sayama K, Arakawa H (2002) Photocatalytic hydrogen and oxygen formation under visible light irradiation with M-doped InTaO<sub>4</sub> (M = Mn, Fe, Co, Ni and Cu) photocatalysts. *J Photochem Photobiol A Chem* 148:65–69. [https://doi.org/10.1016/S1010-6030\(02\)00068-0](https://doi.org/10.1016/S1010-6030(02)00068-0)
- Zou Y, Hu Y, Shen Z et al (2022) Application of aluminosilicate clay mineral-based composites in photocatalysis. *J Environ Sci* 115:190–214. <https://doi.org/10.1016/J.JES.2021.07.015>
- Zuas O, Abimanyu H, Wibowo W (2014) Synthesis and characterization of nanostructured CeO<sub>2</sub> with dyes adsorption property. *Process Appl Ceram* 8:39–46. <https://doi.org/10.2298/PAC1401039Z>

**Publisher's Note** Springer Nature remains neutral with regard to jurisdictional claims in published maps and institutional affiliations.